Final Report

Development of Multimodal Traffic Signal Control

Hesham A. Rakha
Virginia Tech Transportation Institute
3500 Transportation Research Plaza
Blacksburg, VA 24061
Tel: 540-231-1505; Fax: 540-231-1555; Email: hrakha@vt.edu

Kyoungho Ahn
Virginia Tech Transportation Institute
3500 Transportation Research Plaza
Blacksburg, VA 24061
Tel: 540-231-1500; Fax: 540-231-1555; Email: Kahn@vt.edu

Date
May 2019

Prepared for the Urban Mobility & Equity Center, Morgan State University, CBEIS 327, 1700 E. Coldspring Lane, Baltimore, MD 21251

ACKNOWLEDGMENT

This effort was funded by the Urban Mobility and Equity Center (UMEC).

Disclaimer

The contents of this report reflect the views of the authors, who are responsible for the facts and the accuracy of the information presented herein. This document is disseminated under the sponsorship of the U.S. Department of Transportation's University Transportation Centers Program, in the interest of information exchange. The U.S. Government assumes no liability for the contents or use thereof.

1. Report No. UMEC-005	**2. Government Accession No.**	**3. Recipient's Catalog No.**
4. Title and Subtitle Development of Multimodal Traffic Signal Control		**5. Report Date**
		6. Performing Organization Code
7. Author(s) *Include ORCID #* Hesham A. Rakha https://orcid.org/0000-0002-5845-2929 Hossam M. Abdelghaffar		**8. Performing Organization Report No.**
9. Performing Organization Name and Address Virginia Tech Transportation Institute 3500 Transportation Research Plaza Blacksburg, VA 24061		**10. Work Unit No.**
		11. Contract or Grant No. 69A43551747123
12. Sponsoring Agency Name and Address US Department of Transportation Office of the Secretary-Research UTC Program, RDT-30 1200 New Jersey Ave., SE Washington, DC 20590		**13. Type of Report and Period Covered** Final
		14. Sponsoring Agency Code

15. Supplementary Notes

16. Abstract

Traffic congestion affects traveler mobility and also has an impact on air quality, which negatively affects public health. Sustainable mobility could enhance air quality and alleviate congestion. Accordingly, optimizing the utilization of the available infrastructure using advanced traffic signal controllers has become necessary to mitigate traffic congestion in a world with growing pressure on financial and physical resources. Hence, this work develops a novel real-time adaptive multi-modal decentralized traffic signal controller that integrates connected vehicles using a Nash bargaining game-theoretic framework by optimizing total queue length. This framework has a flexible phasing sequence and free cycle length, and thus can adapt to dynamic changes in traffic demand. The controller was implemented and evaluated using INTEGRATION microscopic traffic assignment and simulation software. The proposed controller was tested and compared to state-of-the-art isolated and coordinated traffic signal controllers. The developed controller integrates transit signal priority and freight signal priority to maximize flows in real-time using data collected from vehicles through vehicle-to-infrastructure wireless communications. The proposed controller was tested on an isolated intersection, arterial network, and large-scale networks. The simulation results demonstrate that the proposed decentralized controller reduces traffic congestion, fuel consumption and vehicle emission levels, and produces major improvements over other state-of-the-art centralized and de-centralized traffic signal controllers.

17. Key Words: Adaptive traffic signal controller, Decentralized controller, Game theory	**18. Distribution Statement**

19. Security Classif. (of this report) : Unclassified	**20. Security Classif. (of this page)** Unclassified	**21. No. of Pages** 69	**22. Price**

Contents

List of Figures

List of Tables

Abstract

Traffic congestion affects traveler mobility and also impacts air quality, which negatively affects public health. Sustainable mobility could enhance air quality and alleviate congestion. Accordingly, optimizing utilization of the available infrastructure using advanced traffic signal controllers has become necessary to mitigate traffic congestion in a world with growing pressure on financial and physical resources. Hence, a novel real-time adaptive multi-modal decentralized traffic signal controller that integrates connected vehicles is developed here using a Nash bargaining game-theoretic framework by optimizing total queue length. This framework has a flexible phasing sequence and free cycle length, and thus can adapt to dynamic changes in traffic demand. The controller was implemented and evaluated using INTEGRATION microscopic traffic assignment and simulation software.

The proposed controller was tested and compared to state-of-the-art isolated and coordinated traffic signal controllers. The proposed controller was tested on an isolated intersection, producing a reduction in the queue length ranging from 58% to 77%, and a reduction in vehicle emission levels ranging from 6% to 17%. In arterial testing, the controller was compared to an optimum fixed-time coordinated plan; an actuated controller; a centralized adaptive phase split controller; a decentralized phase split and cycle length controller; and a fully coordinated adaptive phase split, cycle length, and offset optimization controller to evaluate its performance. On the arterial network, the proposed controller produced reductions in the total delay ranging from 36% to 67%, and a reduction in vehicle emissions ranging from 6% to 13%. Statistical tests show that the proposed controller produces major improvements over other state-of-the-art centralized and decentralized controllers.

The developed controller integrates transit signal priority and freight signal priority to maximize flows in real-time using data collected from vehicles through vehicle-to-infrastructure wireless communications. Integrating the transit signal priority in the developed controller on an isolated intersection resulted in an improvement in the average vehicle travel time of 77.5%, average passenger travel time of 76.8%, average total delay of 56.6%, average stopped delay of 72.7%, average fuel consumption of 14.5%, and average emissions of 17.6%. In addition, the results of integrating the freight signal priority in the developed controller on an isolated intersection showed improvements in average vehicle travel time of 78.8%, average total delay of 50%, average stopped delay of 69%, fuel consumption of 13.3%, and emissions of 16%.

In the domain of large scale networks, simulations were conducted in Blacksburg, Virginia, on an road network composed of 38 signalized intersections. The results showed significant reductions in the intersec-

tion approaches, with travel time savings of 23.6%, a reduction in the average queue length of 37.6%, a reduction in the average number of vehicle stops of 23.6%, a reduction in CO_2 emissions of 10.4%, and a reduction in the fuel consumption of 9.8%. The proposed controller was also tested on a road network in downtown Los Angeles, California, including the most congested downtown area, with 457 signalized intersections, and the results were compared to the performance of a decentralized phase split and cycle length controller. The results showed significant average travel time reductions on the intersection links of 35.1%, a reduction in the average queue length of 54.7%, a reduction in the average number of stops of 44%, a reduction in CO_2 emissions of 10%, and a reduction in the fuel consumption of 10%. Furthermore, simulations were conducted at lower traffic flow levels and results showed significant improvements in the network's performance, producing reductions in vehicle average total delay of 36.7%, a reduction in the stopped delay of 90.2%, and a reduction in the average number of stops of 35% compared to a decentralized phase split and cycle length controller.

The results demonstrate that the proposed decentralized controller reduces traffic congestion, fuel consumption, and vehicle emission levels, and produces major improvements over other state-of-the-art centralized and decentralized controllers.

1 Introduction

Traffic growth constrained by available capacity in urban areas affects traveler mobility, air quality, and public health [1]. Reducing traffic congestion can improve these conditions while simultaneously decreasing transportation-related energy use. In 2013, traffic congestion cost Americans $\$124.2$ billion in direct and indirect losses. This number will increase 50% by 2030, rising to $\$186.2$ billion [2]. In 2013, $\$78$ billion of this loss resulted from time and fuel wasted in traffic (direct costs) and $\$45$ billion was the sum of indirect costs. By 2030, the estimated annual cost of traffic in the U.S. and Europe will soar to $\$293$ billion, a rise of nearly 50% from 2013.

Sustainable mobility can help reduce traffic congestion and vehicle emissions. Accordingly, optimizing the utilization of the available infrastructure using advanced traffic signal controllers has become increasingly necessary to mitigate traffic congestion in a world with growing pressure on financial and physical resources. A signalized intersection is designed (controlled) to allow traffic flow to proceed efficiently and safely by separating conflicting movements in time rather than in space. Traffic signal controllers attempt to minimize various traffic parameters (e.g., delay, queue length, and energy and emission levels) by optimizing traffic signal control variables that include the cycle length, phase scheme and sequence, phase split, and offset. Consequently, traffic signal optimization algorithms attempt to identify the optimal values of one or more traffic signal control variables for specific traffic conditions. Most currently implemented traffic signal systems fall into one of the following categories: fixed-time plan (FP), actuated (ACT), responsive, or adaptive [3].

An FP system is developed off-line using historical traffic data to compute traffic signal timings; real-time traffic data is not considered. Thereafter, the order and duration of all phases remain fixed and do not adapt to fluctuations in traffic demand. As a result, FP systems are known to age with time, and are primarily suitable for relatively stable and regular traffic flows.

ACT traffic signal controls, on the other hand, respond to changes in traffic demand patterns using local actuations. This type of control requires that vehicle detectors be installed at intersection approach stop lines. The ACT timing plan responds to traffic demand by placing a call to the controller based on the presence or absence of vehicles approaching or leaving the intersection. Once a call is received, the controller decides whether to extend or terminate the green phase in response to the actuation source. Note, however, that while ACT signal control has been proven to perform better than FP traffic signal control, in most cases, ACT control does not offer any real-time optimization to properly adapt to traffic fluctuations [4].

Adaptive systems use detector inputs, historical trends, and predictive models to predict traffic arrivals at intersections. Using these predictions, they determine the best gradual changes in cycle length, splits, and offsets to optimize an objective function, such as minimizing the delay or the queue length, for intersections within a predetermined sub-area of a network [5]. Examples in this category are the Split Cycle Offset Optimization Tool (SCOOT) and the Sydney Coordinated Adaptive Traffic System (SCATS) systems. The SCOOT system minimizes a performance index that is a function of delay and number of vehicle stops at all approaches in the network [6]. SCOOT performs effectively in under-saturated traffic conditions, and is a macroscopic model that does not capture microscopic behavior such as gap acceptance and lane changing behavior. SCATS monitors the traffic flows and headways at the stop bars [7] based on the volumes and headways gathered in 1-minute intervals; as a result, green times (splits) are reallocated to the phases of greatest need. Other examples of adaptive systems are RHODES (Real-Time, Hierarchical, Optimized, Distributed, and Effective System) [8] and OPAC (Optimized Policies for Adaptive Control) [9], which optimize an objective function for a specified rolling horizon (using traffic prediction models) and have pre-defined sub-areas (limited flexibility) in which the signals can be coordinated. RHODES and OPAC are based on dynamic programming that requires a state transition probability model for the traffic environment, which is difficult to obtain.

One of the main disadvantages of ACT and adaptive traffic control approaches is that their operation is constrained by maximum and minimum values for cycle lengths, splits, and offsets. They also have to go through a pre-defined sequence of phases. In addition, some of today's most sophisticated traffic control systems use hierarchies that either partially or completely centralize the decisions, making the systems more vulnerable to failures in one of the master controllers. In such events, the entire area of influence of the master traffic signal, which may include several intersections, will be compromised by a single failure. Hierarchies also make systems more difficult to scale up, as centralized computers will need to interconnect all intersections within pre-defined subareas, creating limitations and additional requirements as the network is expanded [10].

Traffic flow is highly dependent on factors such as time-of-day, day-of-the-week, weather, and unpredictable events, which can include incidents, special events, work zones [11], etc. Consequently, improvements to traffic control strategies could be made if the control system were able to not only respond to the actual conditions found in the field, but to also adapt their actions to transient conditions.

The objective of this research is to develop a novel adaptive traffic signal controller with the following features to reduce traffic congestion and vehicle emissions by addressing the limitations of existing state-of-

the practice and state-of-the-art adaptive traffic signal controllers: has the ability to adapt the signal timing based on observed traffic state without using historical data; is decentralized, which will increase both the scalability and robustness of the system, and control a large urban traffic network through a number of control agents to avoid the issue of a single point failure in the centralized systems; is model free—doesn't need an explicit model of the environment; has a free cycle length with a flexible phasing sequence; and is designed and evaluated on traffic scenarios that closely represent those found in the real world, which will ensure that the algorithm is not only capable of solving simple traffic problems, but is also applicable to real-life situations.

Game theory is considered a suitable approach with the potential to adapt to traffic fluctuations and randomness of traffic systems, and therefore alleviate traffic congestion more effectively than the more commonly used FP and ACT systems [12]. Game theory studies the interactive cooperation between intelligent rational decision makers, and has been widely used in economic, military, and communication applications. Game theory has also been applied to model traveler route choice behavior [13] and in route guidance [14]. Bargaining theory is related to cooperative games through the concept of Nash bargaining (NB). A bargaining situation is defined as a situation in which multiple players with specific objectives cooperate and benefit by reaching a mutually agreeable outcome. The bargaining process is the procedure that bargainers follow to reach an agreement (outcome), and the bargaining outcome is the result of the bargaining process [15, 16]. The NB solution has been applied in a number of applications, including multimedia resource management [17], allocating multi-user channels to networks [18], a wireless cooperative relaying network [19], investment, wages and employment [20, 21], and for downlink beamforming in an interference channel [22].

To mitigate traffic congestion at signalized intersections, a novel de-centralized traffic signal optimization controller is developed considering a flexible phasing sequence and free cycle length (offering a new, less restrictive perspective to accommodate changes in traffic conditions) using a NB game-theoretic framework (DNB controller). While it is desirable to compare the developed DNB controller to the state-of-the-practice systems, it is difficult to identify a benchmark with available operational details due to intellectual property restrictions, given that the algorithmic details are proprietary. However, it is possible to compare the DNB controller's performance to the operation of an optimum FP controller, an ACT controller, a centralized adaptive phase split (PS) controller, a decentralized phase split and cycle length (PSC) controller [4], and a fully coordinated adaptive phase split-cycle length and offset (PSCO) optimization controller [23, 24] in order to evaluate the proposed DNB controller's performance.

To evaluate the performance of the DNB controller, each of the following was calculated per movement for a signalized intersection: average travel time, average stopped delay, average queue length, average vehicle speed, average vehicle throughput, average fuel consumption, and average emission levels.

The proposed controller was implemented and evaluated in INTEGRATION microscopic traffic assignment and simulation software [25–27]. INTEGRATION is a microsopic model that replicates vehicle longitudinal motion using the Rakha-Pasumarthy-Adjerid collision-free car-following model, also known as the RPA model [28]. The RPA model captures vehicle steady-state car-following behavior using the Van Aerde model [29, 30]. Movement from one steady state to another is constrained by a vehicle dynamics model described in [31, 32]. Vehicle lateral motion is modeled using lane-changing models described in [27]. The model estimates of vehicle delay are validated in [33], while vehicle stop estimation procedures are described and validated in [34]. Vehicle fuel consumption and emissions are modeled using the VT-Micro model [35–37].

Then, the proposed controller was compared to FP and ACT controllers to evaluate its performance at different traffic demand levels. In addition, the DNB controller was implemented and evaluated on an arterial network with six intersections, and was compared to FP, PS, PSC, and PSCO controllers to evaluate its performance. Analysis of variance (ANOVA), Tukey, and pairwise comparison tests were conducted to examine the statistically significant difference of the proposed controller. Moreover, the proposed controller was implemented and evaluated on large scale networks with 38 and 457 intersections. The research methodology is shown in Figure 1.

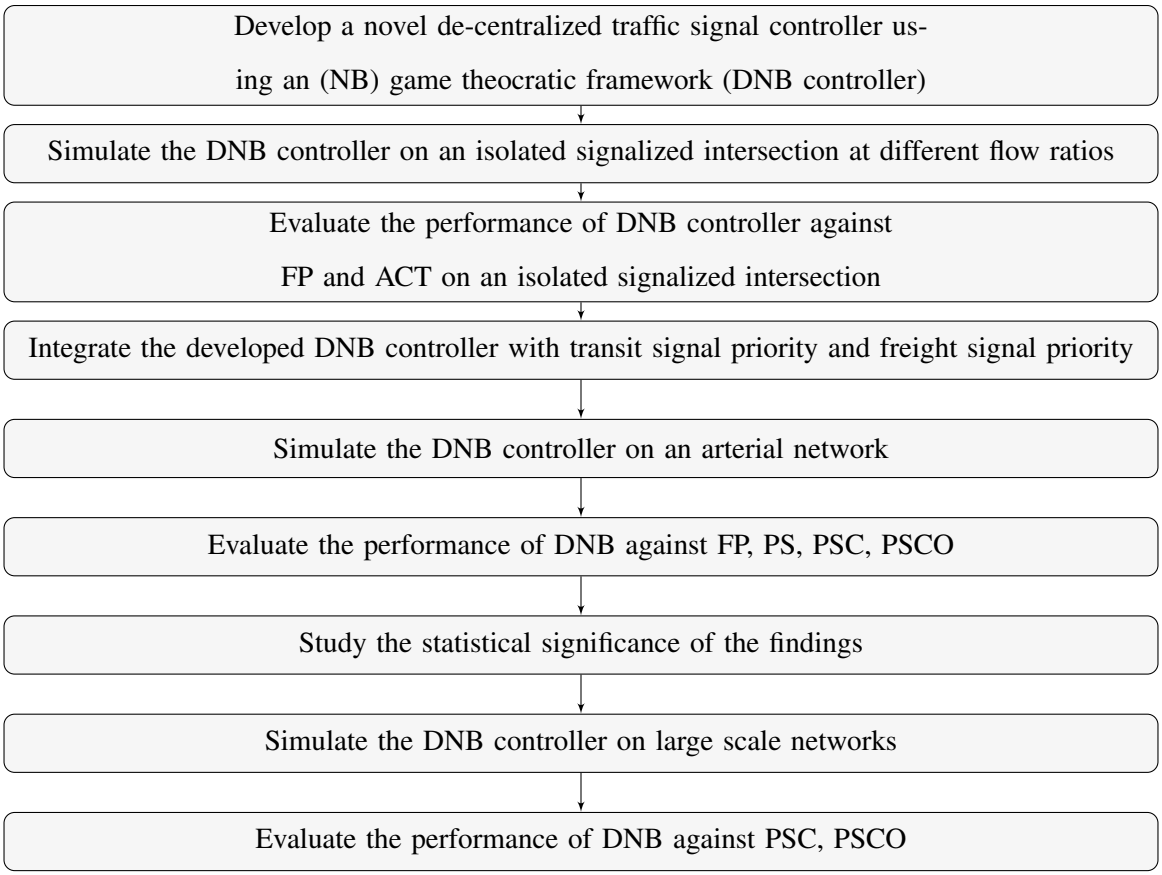

Figure 1: Research methodology

2 Literature Review

A signalized intersection is designed (controlled) to allow traffic flow to proceed efficiently and safely by separating conflicting movements in time rather than in space. Traffic signal controllers attempt to minimize various traffic parameters (e.g., delay, queue length, and energy and emission levels), by optimizing traffic signal parameters, including the cycle length, phase scheme, phase split, and offset. Consequently, traffic signal optimization algorithms attempt to identify the optimal values of one or more traffic signal parameters for specific traffic conditions.

Traffic signal timing parameters could be identified as being in one of two categories: local intersection timing parameters and coordinated operation timing parameters [38]. The phase minimum or yellow change times are examples of local intersection timing parameters. The intersection cycle length, offset, and split are examples of coordination timing parameters. Timing traffic signals in corridors is a multi-objective problem, in which optimizing the solution to one variable can often work to the detriment of another. For

example, optimizing the timings relative to the arterial green band can cause excessive delay on side streets. Conversely, optimizing solely on the basis of network delay does not ensure an adequate green band on the arterial.

The traffic signal controller can be categorized as centralized or decentralized, where decentralized systems offer many advantages over centralized control systems [39]. Decentralized systems are computationally less demanding, as they only require and maintain the relevant information from the surrounding intersections/controllers. Robustness is guaranteed in a decentralized control system, because if one or more controllers fail, the remaining controllers can take over some of their tasks. Decentralized systems are scalable and easy to expand by inserting new controllers into the system. Decentralized systems are also often inexpensive to establish and operate, as there is no essential need for a reliable and direct communication network between a central computer and the local controllers in the field.

Traffic simulation is the modeling of vehicle traffic systems for the purpose of investigating or planning transportation systems. These simulations offer a safe and convenient environment to investigate possible modifications to transportation systems. Traffic simulation models as a whole can be divided into two broad approaches—microscopic and macroscopic—with the mesoscopic approach being a hybrid of the two. Microscopic simulation relies on individual driver behavior. Each vehicle within the simulation environment is updated discretely using car-following behavior to model the interaction of a vehicle and the preceding vehicle while traveling, considering behaviors such as gap acceptance and lane changing behavior. Instead of modeling individual vehicle behavior, macroscopic traffic simulation models rely on traffic flows, densities, and speed to model transportation systems. While macroscopic traffic flow models describe the behavior of a stream of vehicles along a roadway stretch, microscopic car-following models describe the behavior of a pair of vehicles within a traffic stream. Mesoscopic traffic simulation models combine elements of both macroscopic and microscopic traffic simulation. They typically model individual vehicles (a microscopic approach); however, the actions of these vehicles are based on overall averages (a macroscopic approach).

Most currently implemented traffic signal systems fall into one of the following categories: FP controllers, actuated controllers, or adaptive controllers.

Fixed-time Plan

An FP controller is developed off-line using historical traffic data to compute traffic signal timings; real-time traffic data is not considered. Thereafter, the order and duration of all phases remain fixed and do not adapt to fluctuations in traffic demand. As a result, these plans are known to age with time. As such, they are suitable for relatively stable and regular traffic flows. The traffic system is a dynamic system; one particular

predefined traffic signal plan cannot efficiently fit all real-time traffic conditions [40]. Examples of software that compute fixed-time signal timing include TRANSYT-7F and PASSER. TRANSYT-7F (TRAffic Network StudY) is a macroscopic deterministic optimization and simulation model that considers platoons of vehicles instead of individual vehicles. The model attempts to minimize a disutility index based on delay, stops, and queue lengths [41]. This approach has been found to only be appropriate for under-saturated conditions [42].

PASSER (Progression Analysis and Signal System Evaluation Routine) is an arterial-based, bandwidth optimizer (i.e., it maximizes the green band to move the anticipated platoon of vehicles through the arterial signal system without stopping) that computes phase sequences, cycle lengths, and offsets for a maximum of 20 intersections in a single run [42]. PASSER works within a given cycle length and split to find offsets that maximize an arterial green band.

Actuated Control

ACT traffic signal control, on the other hand, responds to changes in traffic demand patterns by implementing a window of green time (minimum green to maximum green) as opposed to the fixed green time in an FP system. This type of control requires that vehicle detectors be installed at approach stop lines to the intersection. The ACT timing plan responds to traffic demand by placing a call to the controller regarding the presence or absence of vehicles approaching or leaving the intersection, respectively. Once a call is received, the controller decides whether to extend or terminate the green phase in response to the actuation source.

ACT control schemes have maximum green times equal to FP control systems. When traffic flows are consistently high, ACT control operates as FP control. ACT control can also be operated as semi-ACT control, where detectors are only placed on minor streets, and is best suited for locations where local minor streets intersect with arterials. Note, however, that while ACT signal control has been proven to perform better than FP traffic signal control in most cases, ACT traffic signal control does not offer any real-time optimization to properly adapt to traffic fluctuations. Consequently, ACT signal control is less sensitive to the traffic demand (i.e., number of vehicles) calling for the actuation and might result in very long queues in grid-like networks [4].

Adaptive Controllers

Adaptive traffic signal systems use detector inputs, historical trends, and predictive models to predict traffic arrivals at intersections. Adaptive systems have the potential to efficiently alleviate traffic congestion by adjusting the signal timing parameters in response to traffic fluctuations [3]. Using these predictions, they

determine the best gradual changes in cycle length, splits, and offsets to optimize an objective function, such as minimizing the delay or the queue length, for intersections within a predetermined sub-area of a network [5].

State-of the-Practice:

- **Centralized and off-line:** A library of pre-stored signal control plans are implemented. These plans are developed off-line on the basis of historical traffic data, such as morning peak, off-peak, afternoon peak, evening period, midnight period, and the day of week (e.g., weekday vs. weekend, Monday vs. Friday, etc.). Examples in this category include TR2 (Traffic Responsive Control Mode 2) [43], and UTCS-1 (Urban Traffic Control System-First Generation) [44]. Pre-timed plans age with time as traffic flows change. The optimization of the signal timings is conducted off-line, so it is incapable of handling stochastic variations in traffic patterns from day to day.

- **Centralized and on-line:** Controllers in this category are implemented using on-line optimization methods to dynamically adjust the signal timings (offsets, cycle time and splits) by utilizing on-line surveillance information systems. Examples in this category include the SCOOT and SCATS systems. SCOOT was developed in the UK in 1982. It minimizes a performance index that is a function of delay and number of vehicle stops at all approaches in the network [6]. SCOOT performs effectively in under-saturated traffic conditions, and is a macroscopic model that does not capture microscopic behavior, such as gap acceptance and lane changing behavior. SCATS was developed in Australia in 1963, It monitors the traffic flows and headways at the stop bars [7] based on the volumes and headways gathered in one-minute intervals. Green times (splits) are reallocated to the phases of greatest need (i.e., in a hierarchical system). Traffic progression along corridors is achieved in a centralized fashion that relies on communication often not scalable to expand the size of the network, is relatively complex to operate with many parameters to be adjusted by a human operator, and is expensive.

- **De-centralized and on-line:** Controllers in this category are decentralized, computationally less demanding, robust, scalable, inexpensive, and use dynamic programming that captures the stochastic nature and dynamics of the traffic system. Examples in this category are RHODES [8] and OPAC [9]. OPAC was the first to recognize the need to migrate from parametric models, which optimize parameters such as cycle time, splits, and offsets, to non-parametric models, in which the decision to switch between phases is based on actual arrival data at the intersection. OPAC uses two levels of control in

a decentralized fashion: a local level and a network level. At the local control level, OPAC determines the next phase at the intersection. At the network control level, OPAC provides progression. RHODES optimizes an objective function for a specified rolling horizon (using traffic prediction models) and has pre-defined sub-areas (limited flexibility) in which the signals can be coordinated. RHODES and OPAC are based on dynamic programming that require a state transition probability model for the traffic environment, which is difficult to obtain. The number of states that could represent wide traffic conditions is typically massive. Therefore, dynamic programming algorithms are computationally intractable [45].

Although existing adaptive traffic systems offer improvements in performance over FP and ACT controllers, they still suffer from combinations of the following limitations:

- Operation is constrained by maximum and minimum values for cycle lengths, splits, and offsets.
- Centralization limits the scalability and robustness of the overall system in cases of communication failure.
- They are expensive to install and maintain [46].
- Complexity of the system increases exponentially with the number of intersections [10].
- They require an accurate traffic modeling framework.

State-of the-Art:

Different intelligent techniques have been investigated in the domain of traffic signal optimization domain, and are still under continuous research and development.

- **Genetic Algorithm:** The genetic algorithm is known to be an algorithm for locating the best optimal solution throughout the evolutionary process of the possible solutions [47]. The problem is modeled as an imitated biological environment, where all the possible solutions are treated as individual chromosomes in a population [48]. The concept of a genetic algorithm allows the population of solutions to compete and survive throughout the evolution, and only the fit and strong solutions will survive at the end of the evolution process [49]. In genetic-algorithm-based optimization traffic signal timing management, a chromosome contains the intersection's signal timing parameters, such as cycle length, green split, phase sequence, and offset, as these are the parameters which tend to be optimized [50], [51]. Chin et al. [52] proposed a fitness function to evaluate the individual chromosomes based on traffic delay and fluency on two intersections with a single lane on each link. They used a selection algorithm that combined a ranking and elitist selection method.

Vogel et al. [53], applied an approach that evolved three chromosomes (phase, phase order, green), to encode the various parameters necessary to define the traffic signal plan for an isolated intersection. Phase chromosomes encode which flow directions belong to each phase, where the number of chromosomes used depends on the number of phases, which can range from 2 to the number of flow directions. Phase order chromosomes encode the order in which the phases of the signal plan occur. Green time chromosomes contain the amount of green time that should be allocated for each phase. Genetic algorithms can solve simple networks and deal with static traffic volumes. However, as the networks increase in size, the search space involved in finding effective signal plans will increase significantly, and a large amount of centralized computing power is required. Genetic algorithms are a biomimetic method for global optimization, and are not apt to be trapped in local optima because of their characteristics of random search and implicit parallel computing. However, encountering a large-scale problem, this method will spend an inordinate amount of time to converge to the optima, which is disadvantageous for on-line optimization of area traffic coordinated control. Moreover, the convergence rate is sensitive to the parameters selected, which depend on practical problems to be solved. Thus, the application of the genetic algorithm to area traffic coordinated control is limited [54]. In addition, it is not certain that the local solution obtained is also the global optimum [55].

- **Fuzzy Logic:** The idea of fuzzy logic was first proposed by Zadeh [56], who posited that truth values of variables can take on a continuous value in the range of $]0;1[$, as opposed to the traditional binary truth values of 0 or 1. Decisions in fuzzy logic are usually made using a rule base, which can be developed using expert knowledge, trial-and-error, or an automatic method such as a genetic algorithm.

  A fuzzy traffic signal controller uses linguistic rules in the following form: if variable1 is value1 then output (e.g., if the approaching traffic volume is large and the queuing traffic volume is small, then the green signal is long). The performance of the controller greatly relies on the effectiveness of the rules developed and it can be difficult to determine if the rules being used are efficient.

  The first application of fuzzy logic in the traffic signal control domain was proposed by Pappis [57] for an isolated intersection. This approach consisted of three input variables: time (very short, short, medium, long, and very long), recent arrivals at the green phase (none, few, medium, many, too many) and queue length at the red phase (very small, small, small plus, long, very long). The rule base, which was developed by trial-and-error in this case, produces a single output from these inputs, which is the

extension time for the current phase. As opposed to using the extension principle, Chiu and Chand [58], designed a controller which adjusts phase split, offset, and cycle length, where the rule base remains static and does not adapt along with changing traffic parameters, which can lead to degraded performance over time, as the system does not generate a predictive model of traffic.

Membership functions are the building blocks of fuzzy set theory (i.e., fuzziness in a fuzzy set is determined by its membership function). Accordingly, the shapes of membership functions are important for a particular problem since they have an effect on a fuzzy inference system. The concepts large, small, and long are fuzzy sets. That is, they are not precise, and elements belonging to one set may partially belong to some other set too. For example, a measurement of five vehicles is small to some degree and also large to some other degree. Most fuzzy traffic signal controllers are not adjustable. In other words, the parameters of the fuzzy controller remain the same in changing traffic situations. Most researchers work at control at an isolated intersection. A traffic coordinated control system is a complex large-scale system with many interacting factors, and it is more appropriate to use fuzzy control methods for traffic signal control of the isolated intersection [54].

- **Machine Learning:** The neural-network-based control signal depends on a set of weighted coefficients, which must be estimated. Once these weights are properly specified, the control signal takes state information on traffic conditions at any given time and produces optimal instantaneous signal light timings. Spall et al. [59], presented an approach for optimal light timing based on a neural network serving as the basis for the control law, with the weight estimation occurring in closed loop mode via the simultaneous perturbation stochastic approximation algorithm, by which the neural network controller weights are estimated (trained) at least once a day. This approach was illustrated by simulation on a six-intersection network with moderate congestion. This model had two shortcomings. First, the approach involved the use of heuristics to manually identify the general traffic patterns (morning and evening peaks) and the assignment of time periods for each pattern. The robustness of the system may come into question if the fluctuations of the traffic volume in the traffic network are not periodic. Second, a neural network is assigned to each time period, and the weights of the neural network are updated only during the duration of the time period. This implies that the weight update is done only on a daily basis whenever the same traffic pattern and time period arises. As such, the traffic controllers may not be able to respond well to changes in the traffic network within the same time period. The neural network has to be re-updated time and again to take into consideration

changes in the long-term dynamics of the traffic network even after the convergence. Srinivasan et al. [60], strove to avoid the limitations of [59] by developing a distributed unsupervised traffic responsive signal controller using a neurofuzzy algorithm.

Various approaches have been proposed for designing real-time traffic signal controllers using neural networks. Most of these works are based on the distributed approach, where an agent is assigned to update the traffic signals of a single intersection based on the traffic flow in all the approaches of that intersection. The effectiveness of the proposed neural controller for controlling a large-scale traffic network with multiple intersections cannot be established. Neural networks adapt very slowly to changing traffic parameters, where online learning has to take place continuously once the agent-based traffic signal controllers are implemented into the traffic network. Some works require multiple models to be maintained for various times within a day. The inner-workings of neural networks are often hard for humans to understand.

Reinforcement learning (RL) is inspired by behavioral psychology. It is a machine learning approach which allows agents to interact with the environment, attempting to learn the optimal behavior based on the feedback received from interactions. The feedback may be available right after the action, or several time steps later, which makes the learning more challenging [61]. This typically involves breaking the environment into states, from which each agent can select a possible action. The reward gained from taking an action within a state determines the level of reinforcement, which in turn affects the likelihood that the agent will select that action when it is next in that state. RL is based on the idea that if an action has good consequences, then the tendency to produce that action is strengthened [62].

Wiering [63] utilized model-based RL with state transition models and state transition probabilities to control traffic-light agents to minimize vehicle waiting time in a small grid network. In that study, agents correspond to the traffic signals but the learning task is designed such that the state representation is a function of the waiting time for individual vehicles (i.e., vehicle-based state representation) aggregated over all vehicles around the intersection. The network is discretized into a number of lanes and each lane is discretized into possible places for cars, which are referred to as cells. As a result, the number of states grows with the number of lanes and the number of vehicles occupying each cell in a lane. Therefore, the number of states grows intractably with the network size and traffic volume, which makes it impractical to implement in medium or large-scale traffic networks. Even for relatively small networks, the number of states will increase exponentially with the increase in the

number of vehicles, resulting in slow convergence speed. Abdulhai et al.[64], applied a model-free Q-learning technique to a simple two-phase isolated traffic signal in a two-dimensional road network. According to the state information that includes the queue lengths on the four approaches, the agent chooses to either remain in the current phase or to change it, with the goal of minimizing the average number of waiting vehicles in all approaches. In the uniform and constant profile cases, Q-learning either slightly outperformed or was equal to the pre-timed control.

Salkham et al. [65] applied a Q-learning strategy that allowed an agent to exchange rewards with its neighbors on 64 signalized intersections. The state-action space was simple and very time coarse. Each agent decided the phase splits every two cycles, which did not capture the rapid dynamics of congestion—coordination between the agents' actions was missing.

Studies have considered the use of RL algorithms for traffic control, but they are very limited in terms of network complexity and traffic loadings, so that realistic scenarios, over saturated conditions, and transitions from under saturation to over saturation (and vice versa) have not been fully explored. Many questions remain about the adequate management of RL agents when traffic demands are not balanced (in terms of volume, number of lanes, and link length), when the demand changes over time, and when the volumes exceed the capacity of the network so that the signal control should prevent queue overflows. The advantage of reinforcement learning is that it is not necessary to establish a mathematical model for the external environment. However, there is also a disadvantage in that it converges slowly.

- **Feedback Control:** Ekbatani et al. [66, 67], developed a strategy that exploits the network fundamental diagram for urban networks to improve mobility in saturated traffic conditions via application of gating measures, based on simple feedback control structure (PI controller). The idea is to hold traffic back (via prolonged red phases at traffic signals) upstream of the links to be protected from over-saturation, whereby the level or duration of gating may depend on real-time measurements from the protected links, which may result in a long queue and delays at the gate. Gating at the border of the network may not be applicable if there are no proper links to store the gated vehicles (queuing), or if there are an insufficient number of signalized junctions.

  The linear quadratic controller (LQR) controller is a well-known controller for minimizing cost functions. The LQR controller has been tested and proven to be effective [68, 69]. Konstantinos et al. [70] addressed the problem of real-time traffic signal control using an LQR controller that minimized

and balanced the relative occupancies of the network links using a simplified continuity equation. The proposed strategy didn't capture driver behavior or the car-following behavior that modeled the interaction of a vehicle and the preceding vehicle. Neither did this strategy evaluate the performance of the system with the changing traffic volume.

- **Game Theory:** Game theory studies the interactive cooperation between intelligent rational decision makers, and has been widely used in economic, military, and communication applications. Game theory has also been applied to model traveler route choice behavior [13] and in-route guidance [14].The literature indicates that investigation of game-theoretic traffic signal control is very limited. Bargaining theory is related to cooperative games through the concept of Nash bargaining (NB). A bargaining situation is defined as a situation in which multiple players with specific objectives cooperate and benefit by reaching a mutually agreeable outcome. The bargaining process is the procedure that bargainers follow to reach an agreement (outcome), and the bargaining outcome is the result of the bargaining process [15, 16]. The NB solution has been applied in a number of applications, including multimedia resource management [17], allocating multi-user channels to networks [18], a wireless cooperative relaying network [19], investment, wages and employment [20, 21], and for downlink beamforming in an interference channel [22].

Summary

This section outlines a number of approaches that have been applied to the domain of traffic signal control. The reviewed literature showed that many methodologies have been proposed to date. It also revealed that the field operations of traffic signals in congested networks and saturated traffic conditions are still under development and that there is still room for new developments.

Various computational intelligence-based approaches have been proposed for designing real-time traffic signal controllers, such as fuzzy sets, genetic algorithm and reinforcement learning, and neural networks. Most of these approaches have implemented and tested the controller on an isolated intersection where the effectiveness of the proposed controllers for controlling a large-scale traffic network with multiple intersections cannot be established. Improved optimization approaches are constantly being developed. There are currently no commercially available off-the-shelf tools to address these problems, and even the literature offers little structured guidance to accomplish this task.

Accordingly, this research attempts to develop a novel traffic signal controller that meets a number of requirements. First, the controller should be able to adapt signal plans based on observed traffic state

without using historical data, which tends to be inaccurate, resulting in inefficient signal plans. Second, the developed control system should be decentralized, which will increase both the scalability and robustness of the system in order to avoid the problems inherent with complex centralized communication. Decentralized systems are often inexpensive to establish and operate, as there is no essential need for a reliable and direct communication network between a central computer and the local controllers in the field. In addition, the developed controller should integrate transit signal priority (TSP) and freight signal priority (FSP) to maximize flows in real-time. Finally, the controller should be designed and evaluated on traffic scenarios that closely represent those found in the real-world, which will ensure that the controller is not only capable of solving simple traffic problems, but is also applicable to real-life situations. This controller should increase the traffic handling capacity of roads, and reduce fuel consumption, thereby decreasing air pollution.

3 Developed Traffic Signal Controller (DNB)

This section presents the developed traffic signal timing controller to alleviate congestion at signalized intersections using an NB game-theoretic framework.

3.1 NB Solution for Two Players

A bargaining situation is defined as a situation in which multiple players with specific objectives cooperate and benefit by reaching a mutually agreeable outcome (agreement). In bargaining theory, there are two concepts: the bargaining process and the bargaining outcome. The bargaining process is the procedure that bargainers follow to reach an agreement (outcome) [71, 72]. Nash adopted an axiomatic approach that abstracts the bargaining process and considers only the bargaining outcome [15]. The bargaining problem consists of three basic elements: players, strategies, and utilities (rewards). Bargaining between two players is illustrated in the bi-matrix shown in Table 1. Each player, P_1 and P_2, has a set of possible actions A_1 and A_2, whose outcome preferences are given by the utility functions u and v, respectively, as they take relevant actions.

Table 1: Two Players Matrix Game

		P_2	
		A_1	A_2
P_1	A_1	$\mathrm{u}_1, \mathrm{v}_1$	$\mathrm{u}_2, \mathrm{v}_2$
	A_2	$\mathrm{u}_3, \mathrm{v}_3$	$\mathrm{u}_4, \mathrm{v}_4$

The space (S), shown in Figure 2, is the set of all possible utilities that the two players can achieve; the vertices of the area are the utilities where each player chooses their pure strategy. The disagreement or the threat point $\mathrm{d} = (\mathrm{d}_1, \mathrm{d}_2)$ corresponds to the minimum utilities that the players want to achieve. The disagreement point is a benchmark, and its selection affects the bargaining solution. Each player attempts to choose their disagreement point in order to maximize their bargaining position. Subsequently, a bargaining problem is defined as the pair (S,d) where $\mathrm{S} \in \mathbb{R}^2$ and $\mathrm{d} \in \mathrm{S}$ such that S is a convex and compact set, and there exists some $s \in \mathrm{S}$ such that $s > \mathrm{d}$. Nash stated the following four axioms that identify properties that the bargaining solution must satisfy:

- Pareto efficiency: at the bargaining outcome, no player can improve without decreasing the other

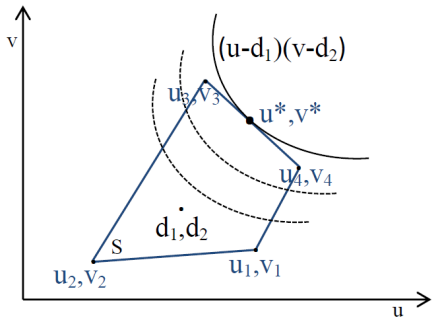

Figure 2: Utility region.

player's utility, i.e., no point $(\mathrm{u}, \mathrm{v}) \in \mathrm{S}$ exists such that $\mathrm{u} > \mathrm{u}^*$ and $\mathrm{v} \geq \mathrm{v}^*$or $\mathrm{u} \geq \mathrm{u}^*$and $\mathrm{v} > \mathrm{v}^*$.

- Symmetry: the bargaining solution would not discriminate among the players if these players were indistinguishable; i.e., if $\mathrm{d}_1 = \mathrm{d}_2$ and S is symmetric around $\mathrm{u} = \mathrm{v}$, then $\mathrm{u}^* = \mathrm{v}^*$.
- Invariance to equivalent utility representation: the bargaining outcome varies linearly if the utilities are scaled using an affine transformation.
- Independence of irrelevant alternatives: if the solution to the bargaining problem lies in a subset $\mathrm{S}'$of S, then the outcome does not change if bargaining is performed on S' instead of S.

Nash's theorem states that there exists a unique solution satisfying the four axioms, and this solution is the pair of utilities $(\mathrm{u}^*, \mathrm{v}^*)$ that solves the following optimization problem:

$$\underset{\mathrm{u,v}}{max}\ (\mathrm{u} - \mathrm{d}_1)(\mathrm{v} - \mathrm{d}_2), \tag{1}$$

$$s.t. (\mathrm{u}, \mathrm{v}) \in \mathrm{S}, (\mathrm{u}, \mathrm{v}) \geq (\mathrm{d}_1, \mathrm{d}_2)$$

The NB solution $(\mathrm{u}^*, \mathrm{v}^*)$ of this optimization problem can be calculated as the point in the bargaining set that maximizes the product of the players' utility gains relative to a fixed disagreement point.

3.2 NB Solution for Multi-players

This section describes the game model and the NB solution for multi-players (N), and shows how the model is adapted (from Section 3.1) and applied to control a multi-phase signalized intersection (DNB controller). First, we use phasing scheme for a four-legged intersection [73], assuming we have four players ($\mathrm{N} = 4$), to represent the intersection phases as shown in Figure 3, with protected, leading main street left-turn phases.

In the game model, the four phases represent the players P_1, P_2, P_3, and P_4 of a four player cooperation game. For each player (phase), there are two possible actions: maintain (A_1) or change (A_2). These actions

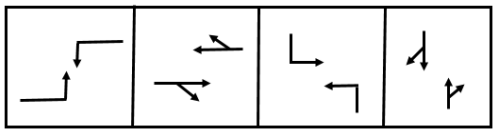

Figure 3: Phasing scheme.

represent the state of the traffic signal [74]. Specifically, maintain indicates that the state of the signal will not change (i.e., if it is green, it will remain green; if it is red, it will remain red.). Change means the state of the signal will change (i.e., if it is green, it will switch to yellow and then red; if it is red, it will become green) in the simulated time interval. The combinations of phases offer four possibilities, where only one player holds the green indication and all others hold red indications.

In the simulation, INTEGRATION traffic simulation software monitors the vehicle speeds and the vehicle flow approaching the intersection and continuously updates them for each lane connected to the signalized intersection. If the vehicle (v) speed (s_v^t) is less than a certain threshold speed (s^{Th}) at time (t), the vehicle is assigned to the queue, and the current queue length associated with the corresponding lane (l) is updated. Once the vehicle's speed exceeds (s^{Th}), the queue length is updated (i.e., shortened by the number of vehicles leaving the queue) and formulated mathematically as

$$q_l^t = \sum_{v \in v_l^t} q_v^t \tag{2}$$

$$q_v^t = \begin{cases} 1 & \text{if } s_v^{t-1} > s^{Th} \ \& \ s_v^t \leq s^{Th} \\ -1 & \text{if } s_v^{t-1} \leq s^{Th} \ \& \ s_v^t > s^{Th} \\ 0 & \begin{cases} \text{if } s_v^{t-1} \leq s^{Th} \ \& \ s_v^t \leq s^{Th} \\ \text{if } s_v^{t-1} > s^{Th} \ \& \ s_v^t > s^{Th} \end{cases} \end{cases} \tag{3}$$

where q_l^t is the number of queued vehicles in lane l at time t.

The utilities (rewards) for each player (phase) in the game can be defined as the estimated sum of the queue lengths in each phase after applying a specific action. The estimated queue length after applying a specific action is calculated according to the following equation:

$$Q_P(t + \Delta t) = \sum_{l \in P} q_l^t + Q_{inl}\Delta t - Q_{outl}\Delta t \tag{4}$$

Where Δt is the updating time interval, q_l^t is the current queue length at time t, $Q_P(t+\Delta t)$ is the estimated queue length after Δt for phase P, Q_{inl} is the arrival flow rate (veh/h/lane), and Q_{outl} is the departure flow rate (veh/h/lane).

The block diagram of applying the DNB controller is shown in Figure 4, where the predefined threat values present an input to the controller. In addition, the flow ratios Q_{inl} and Q_{outl} could be measured by traffic loop detectors. Q_{outl} detectors are generally located at the downstream end of the link, whereas Q_{inl} detectors are located from the downstream end of the link by distances equal to threat points over jam density.

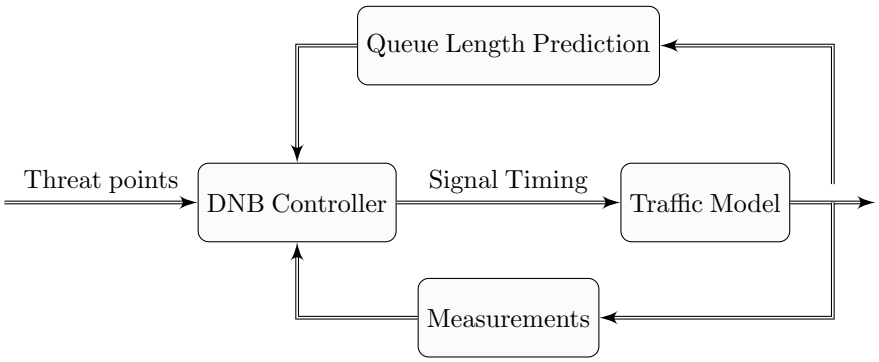

Figure 4: System block diagram.

The objective is to minimize and equalize the queue lengths across the different phases [75, 76]. We use minus queue length as the utility of each strategy. The DNB solution is extended to four players (N=4) with a four-dimensional utility space and disagreement points. The solution for the DNB over the four phase combinations has the following formula:

$$\max_{(\mathrm{u}_1,\ldots,\mathrm{u}_4)} \prod_{i=1}^{\mathrm{N}} (\mathrm{u_i} - \mathrm{d_i}) \tag{5}$$

$$s.t.(\mathrm{u}_1, ..., \mathrm{u}_4) \in S, (\mathrm{u}_1, ..., \mathrm{u}_4) \geq (\mathrm{d}_1, ..., \mathrm{d}_4)$$

The DNB solution can be calculated as the vector that maximizes the product of the player's utility gains relative to a fixed disagreement point.

3.3 Decentralized Mechanism of the DNB Controller

This section presents the decentralized mechanism of the DNB controller on multi-intersections. For the purpose of illustration, we will explain the DNB controller's behavior on three intersections, shown in Table 2.

Assume we have three intersections ($I_1, I_2,\ I_3$), and each intersection has three phases ($Ph_1, Ph_2,\ Ph_3$), where each phase is considered as a player in the game. Hence, each intersection has three players; i.e., I_1 has three players ($P_1, P_2,\ P_3$), I_2 has three players ($P_4, P_5,\ P_6$), and I_3 has three players ($P_7, P_8,\ P_9$). Every intersection has three possible actions (A), where one phase has a green (**G**) period and the others are red (**R**) as illustrated in Table 2.

Table 2: Multi-players Matrix Game

Intersection	First Intersection (I_1)			Second Intersection (I_2)			Third Intersection (I_3)		
Player / **Action**	Ph1(P_1)	Ph2(P_2)	Ph3(P_3)	Ph1(P_4)	Ph2(P_5)	Ph3(P_6)	Ph1(P_7)	Ph2(P_8)	Ph3(P_9)
First	**G**	**R**	**R**	**G**	**R**	**R**	**G**	**R**	**R**
	A_{11}			$\mathbf{A_{21}}$			A_{31}		
Second	**R**	**G**	**R**	**R**	**G**	**R**	**R**	**G**	**R**
	$\mathbf{A_{12}}$			A_{22}			A_{32}		
Third	**R**	**R**	**G**	**R**	**R**	**G**	**R**	**R**	**G**
	A_{13}			A_{23}			$\mathbf{A_{33}}$		

Therefore, for the network of three intersections illustrated in Table 2, there are 27 possible scenarios (action permutations) as shown in Table 3. In order to maximize the overall network performance, we are looking for the best scenario in Table 3.

For Table 2, assume that the first intersection (I_1) has an action ($\mathbf{A_{12}}$) that will maximize its own performance, and intersection (I_2) has an action ($\mathbf{A_{21}}$) that will maximize its own performance, and intersection (I_3) has an action ($\mathbf{A_{33}}$) that will maximize its own performance. Consequently, searching in Table 3 for the best combination yields scenario 12. Therefore, to achieve the maximum network performance, it is sufficient to search for the actions that will maximize an individual intersection's performance. This can also be described using the DNB optimization problem, as shown in the following equations.

Table 3: All possible Network Actions (Permutations)

Scenario #	Network Action
1	A_{11} A_{21} A_{31}
2	A_{11} A_{21} A_{32}
3	A_{11} A_{21} A_{33}
4	A_{11} A_{22} A_{31}
5	A_{11} A_{22} A_{32}
6	A_{11} A_{22} A_{33}
7	A_{11} A_{23} A_{31}
8	A_{11} A_{23} A_{32}
9	A_{11} A_{23} A_{33}
10	A_{12} A_{21} A_{31}
11	A_{12} A_{21} A_{32}
12	$\mathbf{A_{12}}$ $\mathbf{A_{21}}$ $\mathbf{A_{33}}$
13	A_{12} A_{22} A_{31}
14	A_{12} A_{22} A_{32}

Scenario #	Network Action
15	A_{12} A_{22} A_{33}
16	A_{12} A_{23} A_{31}
17	A_{12} A_{23} A_{32}
18	A_{12} A_{23} A_{33}
19	A_{13} A_{21} A_{31}
20	A_{13} A_{21} A_{32}
21	A_{13} A_{21} A_{33}
22	A_{13} A_{22} A_{31}
23	A_{13} A_{22} A_{32}
24	A_{13} A_{22} A_{33}
25	A_{13} A_{23} A_{31}
26	A_{13} A_{23} A_{32}
27	A_{13} A_{23} A_{33}

$$\max_{(u_1,\ldots,u_9)} \prod_{i=1}^{9} (u_i - d_i) \tag{6}$$

$$= \max_{(u_1,\ldots,u_9)} [\underbrace{\prod_{i=1}^{3} (u_i - d_i)}_{I_1} \underbrace{\prod_{i=4}^{6} (u_i - d_i)}_{I_2} \underbrace{\prod_{i=7}^{9} (u_i - d_i)}_{I_3}]$$

$$= \underbrace{\max_{(u_1,\ldots,u_3)} \prod_{i=1}^{3} (u_i - d_i)}_{I_1} \underbrace{\max_{(u_4,\ldots,u_6)} \prod_{i=4}^{6} (u_i - d_i)}_{I_2} \underbrace{\max_{(u_7,\ldots,u_9)} \prod_{i=7}^{9} (u_i - d_i)}_{I_3}$$

It is worth noting that no intersection has to sacrifice its own performance to achieve network optimization. Therefore, the DNB controller is decentralized, which enables it to control a large urban traffic network and avoids the issue of a single point failure as in centralized systems, and also avoids the problems inherent with complex centralized communication. The decentralized behavior of the DNB controller will

increase both the scalability and robustness of the system, whereas other controller systems are associated with exponential increases with the number of intersections when the network is expanded.

The proposed controller was first implemented on an isolated intersection to evaluate its performance, as described in the next section.

4 Isolated Intersection Results

In this section, the DNB solution is applied to obtain the optimal control strategy on an isolated intersection, considering a variable phasing sequence and free cycle length. The system is implemented and evaluated in INTEGRATION microscopic traffic assignment and simulation software. The proposed controller is compared to an optimum FP controller and an ACT controller to evaluate the performance of the proposed DNB controller at different traffic demand levels.

4.1 Experimental Setup

The experiments were tested using the DNB controller on an intersection with four approaches, comprised of three lanes each, located in the heart of downtown Toronto's financial district (intersection of Front and Bay streets) [77] as shown in Figure 5.

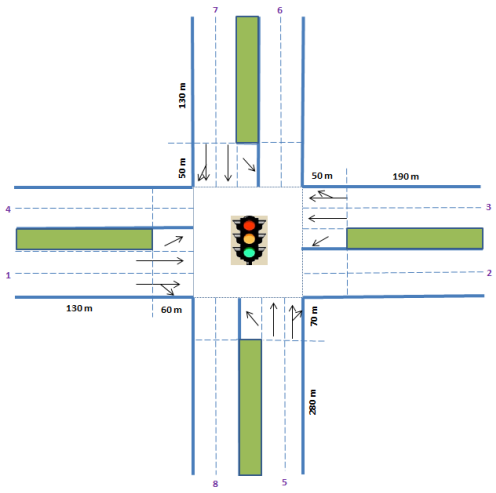

Figure 5: Testbed intersection.

The traffic demand origin-destination (O-D) matrix provided in Table 4 [78], represents the highest total demand approaching the intersection during the afternoon rush hour (PM peak) for the year 2005. The O-D matrix forms an input to INTEGRATION.

The standard NEMA phasing for a four-legged intersection [73] represents the intersection phases as shown in Figure 6, with protected, leading main street left-turn phases. The four phases represent the four players ($\mathrm{N} = 4$) in the game [79].

INTEGRATION software was used to model the intersection [26]. INTEGRATION is a microscopic

Table 4: Origin Destination Demand Matrix

Zone #	2	4	6	8	Total
1	1223	-	134	121	1478
3	-	844	86	278	1208
5	88	71	721	-	880
7	188	100	-	806	1094
Total	1499	1015	941	1205	4660

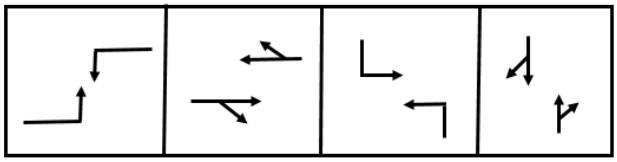

Figure 6: Phasing scheme.

traffic simulation model that traces individual vehicle movements every deci-second. Driver characteristics, such as reaction times, acceleration and deceleration rates, desired speeds, and lane-changing behavior are examples of stochastic variables that are incorporated in INTEGRATION [80].

The following measures of effectiveness (MOEs) were used to evaluate the performance of the system:

- Average Total Delay (s/veh): the sum of delay each deci-second for all vehicles for the entire simulation horizon divided by the number of vehicles.
- Average Stopped Delay (s/veh): the sum of instances where vehicle speed is less than or equal $3.6\mathrm{km/h}$ (pedestrian speed) divided by the number of vehicles.
- Average Queue Length (veh): the sum of vehicles in queue each second divided by the simulation duration.
- Average Travel Time (s): the summation of all trip times divided by the number of vehicles.
- Average Vehicle Speed (km/h): the sum of instantaneous vehicle speeds divided by the number of vehicles.
- Average Throughput (veh/h): the total number of vehicles exiting the intersection divided by the simulation duration.
- Average Fuel (L): the total volume of fuel consumed by vehicles divided by the number of vehicles.
- Average CO2 (grams): the total amount of CO2 produced divided by the total number of vehicles.
- Last Vehicle Arrival Time(s): the arrival time of last vehicle to its destination.

The proposed controller was compared to an optimum FP controller and an ACT controller to evaluate its performance. The FP controller was optimized using the Webster method [40], with a yellow time of 3 s, and all red times of 2 s. The optimized effective green times for the four phases shown in Figure 6 were, 19 s, 47 s, 14 s, 32 s, respectively. ACT control was implemented with minimum green time of 10 s, maximum green time of 78 s, and green extension time of 5 s. The simulations were conducted using the following parameter values: speed at capacity = 60 $(\mathrm{km/h})$, free flow speed = 80 $(\mathrm{km/h})$, jam density = 160 $(\mathrm{veh/km/lane})$, saturation flow rate = 1900 $(\mathrm{veh/h/lane})$, and threshold speed s^{Th}= 4.5 $(\mathrm{km/h})$.

4.2 Experimental Results

An optimum FP and an ACT controller were simulated to serve as benchmarks to evaluate the performance of the DNB controller. Vehicles were allowed to enter the links in the first hour, and the simulation ran for an extra half hour to guarantee that all vehicles exited the network. Three scenarios were simulated: one for the original O-D demand shown in Table 4, the second for a lower demand (L-D), i.e., (-25%) of the original demand, and the third for higher demand (H-D); i.e., $(+25\%)$ of the original demand.

4.2.1 Original Demand (O-D)

The simulation results shown below were obtained using three signal control systems: FP, ACT, and DNB. The MOEs are shown in Table 5 to quantify the effect of each control system on the performance of the signalized intersection.

Five cases were conducted at different threat points (d), and at different updating intervals (Δt) for DNB in order to study their effect on the performance of the DNB algorithm. First, the performance of the intersection using the three control systems (FP, ACT, DNB) was investigated at the following parameter values:

$$Case\ 1 \Rightarrow \mathrm{d} = (-17, -34, -19, -38),\ \Delta \mathrm{t} = 15\mathrm{s}$$

The threat point was chosen based on the number of cars that left-turn pocket lanes could accommodate to prevent spill back into the through lane, where this number was duplicated for the right and the through movements.

The simulation results shown in Table 5 indicate that the DNB controller outperformed the optimum FP and ACT controllers. Since the traffic flow was high on all approaches, no considerable difference was reported between the FP and the ACT controllers. The DNB controller exhibited significant savings in

Table 5: Overall Intersection Performance Measure For Different Control Systems

MOE \ System	FP	ACT	DNB				
			Case 1	Case 2	Case 3	Case 4	Case 5
Average Total Delay (s/veh)	74.268	76.270	32.176	29.390	26.906	43.312	48.148
Average Stopped Delay (s/veh)	46.878	48.77	15.837	13.619	9.553	11.158	25.010
Average Queue Length (veh)	8.294	8.559	2.781	2.484	1.891	2.955	4.623
Average Travel Time (s)	116.141	137.566	53.366	50.577	48.080	74.280	69.879
Average Vehicle Speed (km/h)	21.455	20.617	38.965	38.302	39.954	31.514	31.501
Average Throughput (veh/h)	529.545	529.545	554.762	563.710	563.710	554.762	554.762
Average Fuel (L)	0.1197	0.1212	0.1028	0.1017	0.1037	0.1167	0.1097
Average CO2 (grams)	255.80	258.89	213.708	211.290	213.324	240.083	231.400
Last Vehicle Arrival Time (s)	3852.3	3906.1	3701.1	3664.3	3672.3	3676.4	3693.2

the average total delay, average stopped delay, average queue length, and average travel time. The DNB showed an increase in the average vehicle speed and in the throughput. Subsequently, the performance of the intersection using the proposed DNB controller was investigated using different threat points values and at the same updating interval, using the following parameter values:

$$Case\ 2 \Rightarrow \mathrm{d} = (-17, -55, -19, -51),\ \Delta\mathrm{t} = 15\mathrm{s}$$

In this case, the threat point was chosen based on the number of cars that each phase can accommodate based on the lane lengths, shown in Figure 5, where the right turn and through lanes can accommodate more cars than the left turn lanes. The results in Table 5 show that MOEs in $case\ 2$ outperform the results in $case\ 1$.

Finally, three more simulations were conducted using the proposed DNB algorithm to investigate the effect of the choice of the updating time interval on the algorithm performance using the same threat point values.

$$Case\ 3 \Rightarrow \mathrm{d} = (-17, -55, -19, -51), \Delta\mathrm{t} = 10\mathrm{s}$$

$$Case\ 4 \Rightarrow \mathrm{d} = (-17, -55, -19, -51), \Delta\mathrm{t} = 5\mathrm{s}$$

$$Case\ 5 \Rightarrow \mathrm{d} = (-17, -55, -19, -51), \Delta\mathrm{t} = 20\mathrm{s}$$

The results shown in Table 5 show that $case\ 3$ was superior to the results of the other cases, as well as the FP approach and the ACT approach.

Figure 7 shows the average queue length and the standard deviation across all movements for each control system, (FP, ACT, and DNB). The DNB algorithm resulted in a significant reduction in the queue length.

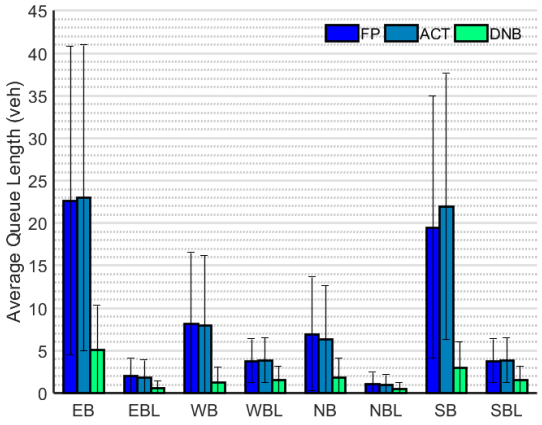

Figure 7: Average queue length.

Figure 8 shows the average values and the standard deviations of the MOEs across all movements over the entire simulation time for each control system, (FP, ACT, and DNB). The DNB algorithm outperformed both FP and ACT for all movements with significant reduction in both the average values and the standard deviations for the total delay, stopped delay, arrival time, fuel consumption, and CO_2 emission. In addition the DNB algorithm resulted in an increase in the average vehicle speed.

The simulation results showed that the DNB controller exhibited major improvements in both the average values and the standard deviations of all MOEs for different movements, which indicates that the system efficiency was improved.

4.2.2 Lower And Higher Demand

To better evaluate the performance of the DNB controller, two other simulations were conducted, one at lower demand (L-D), and the other at higher demand (H-D).

Table 6 shows the results of using the three control approaches at the O-D, L-D, and H-D levels using the following DNB algorithm parameters

$$\mathrm{d} = (-17, -55, -19, -51),\ \Delta \mathrm{t} = 10\mathrm{s}$$

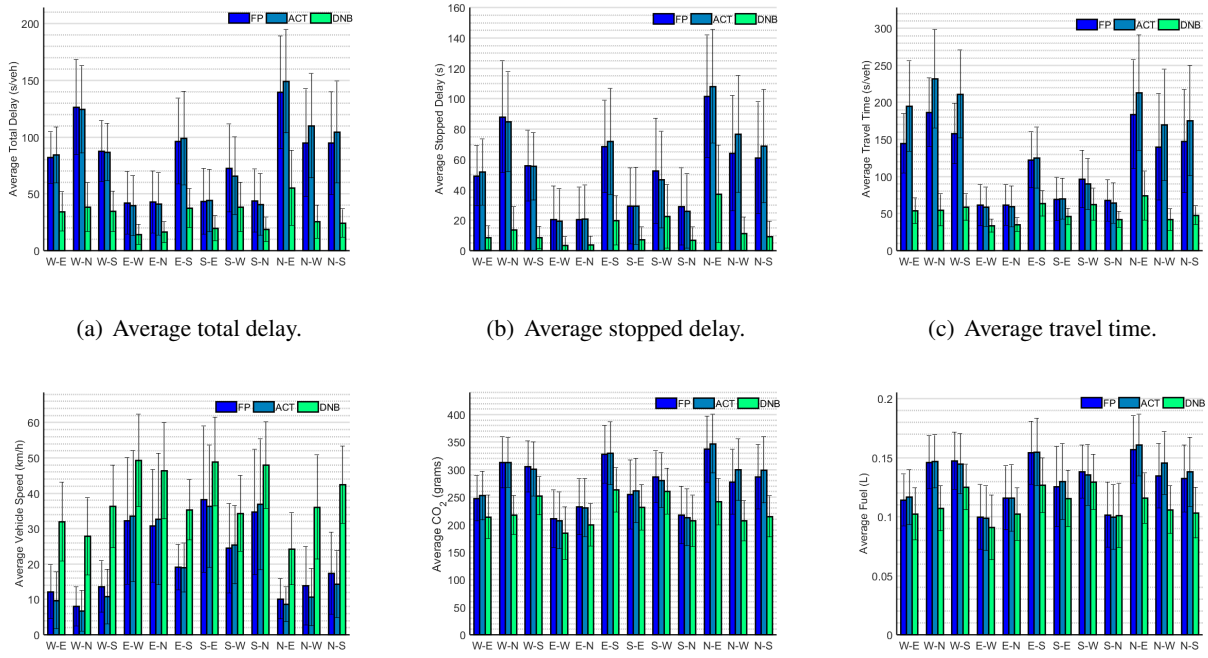

(a) Average total delay.

(b) Average stopped delay.

(c) Average travel time.

(d) Average vehicle speed.

(e) Average CO_2.

(f) Average fuel.

Figure 8: Measures of effectiveness (MOEs).

In addition, Table 6 shows the percent improvement in MOEs using the proposed DNB controller over using either the FP or the ACT approach. The analysis of the results in Table 6 leads to the following findings: the proposed DNB controller outperforms the FP and ACT approaches in terms of average stopped delay, average queue length, average travel time, average vehicle speed, average throughput, average fuel consumed, average CO_2 emitted, and time in which the last vehicle clears the network for different demand levels.

To further investigate the achieved improvements using the DNB controller, simulations were conducted at different flow ratios (Y). The flow ratio can be formulated mathematically as

$$y_i = \frac{v_i}{s_i}, \qquad Y = \sum y_{c,j} \tag{7}$$

where, y_i is the approach flow ratio for lane group i, v_i is the traffic volume, s_i is the saturation flow rate, $y_{c,j}$ is the critical flow ratio for all lane groups that discharge during phase j, and Y is the sum of all critical follow ratios for all phases.

Figure 9 shows the average queue length, the average total delay, and the average CO_2 at different flow ratios; Y ratios vary from 0.1 to 1.2. These results show that significant improvements were achieved using

Table 6: Intersection Performance Measure For Different Control Systems at Different Demand Profiles

Demand	L-D			O-D			H-D		
System / **MOE (Avg)**	FP	ACT	DNB	FP	ACT	DNB	FP	ACT	DNB
Total Delay (s/veh)	41.473	42.913	17.854	74.268	76.270	26.906	101.783	102.938	59.994
Improvement %	56.9503	58.3949		63.7717	64.7227		41.0570	41.7183	
Stopped Delay (s/veh)	27.157	28.222	6.357	46.878	48.77	9.553	62.730	63.679	17.970
Improvement %	76.5917	77.4750		79.6216	80.4121		71.3534	71.803	
Queue Length (veh)	3.5340	3.7087	0.8827	8.2944	8.5593	1.8907	11.4293	11.4806	4.7811
Improvement %	75.0226	76.1992		77.2051	77.9106		58.1680	58.3550	
Travel time (s)	62.602	64.035	38.961	116.141	137.566	48.080	463.612	462.311	228.149
Improvement %	37.7640	39.1567		58.6020	65.0495		50.7888	50.6503	
Vehicle Speed (km/h)	35.759	34.987	47.442	21.455	20.617	39.954	9.600	9.435	21.435
Improvement %	32.6715	35.5989		86.223	93.7915		123.2812	127.186	
Throughput (veh/h)	415.95	415.95	422.66	529.54	529.54	563.71	526.44	532.86	598.56
Improvement %	1.6129	1.6129		6.4516	6.4516		13.6986	12.3287	
Fuel (L)	0.100	0.1017	0.0974	0.1197	0.1212	0.1037	0.1328	0.1337	0.1209
Improvement %	2.6000	4.2281		13.3668	14.4389		8.9608	9.5737	
CO2 (grams)	211.225	214.675	198.15	255.80	258.89	213.32	286.741	288.878	254.40
Improvement %	6.1858	7.6935		16.6052	17.6005		11.2764	11.9327	
Last Vehicle Arrival (s)	3705.2	3706.0	3652.2	3852.3	3906.1	3672.3	4884.8	4876.4	4284.2
Improvement %	1.4304	1.4517		4.6725	5.9855		12.2953	12.1442	

the DNB controller at different traffic volumes.

Figure 10 shows the average queue length at two different flow ratios (Y) (i.e., 0.1 and 1.2). Considerable reductions in the queue lengths were found for all movements.

The simulation results showed that the DNB controller exhibited major improvements in the MOEs for all movements when compared to FP and ACT algorithms, thus improving system efficiency.

4.3 Summary

In this section, the developed DNB controller was applied to an isolated intersection. INTEGRATION microscopic traffic assignment and simulation software was used to evaluate the performance of the controller relative to an optimum FP controller and an ACT controller on a major intersection in downtown Toronto using observed traffic data. Five DNB controller scenarios were simulated considering different update time

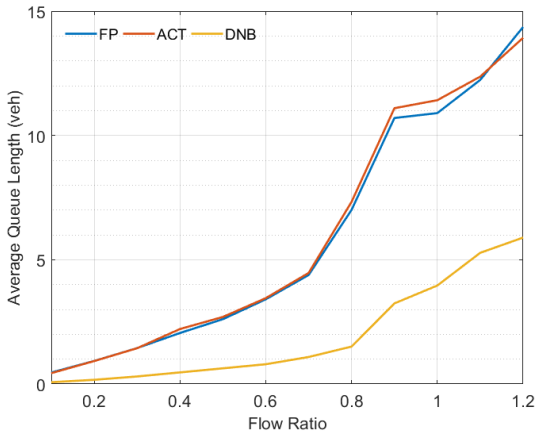

(a) Average queue length.

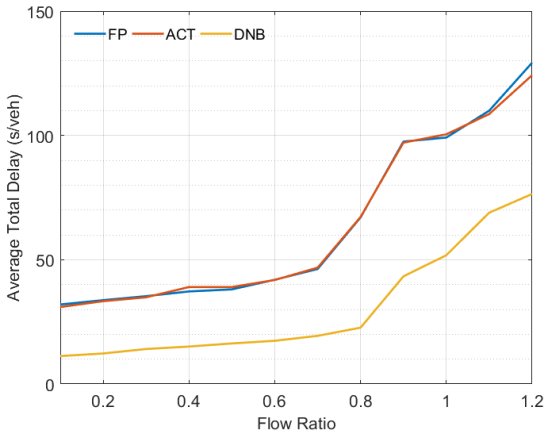

(b) Average total delay.

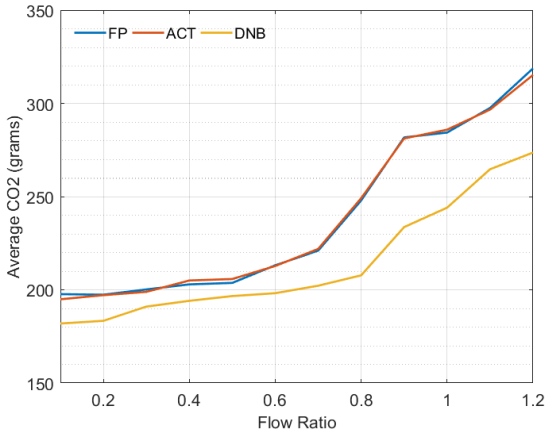

(c) Average CO_2.

Figure 9: Measure of effectiveness vs. flow ratio.

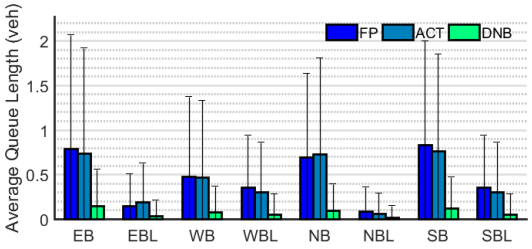

(a) Average queue length at 0.1 flow ratio.

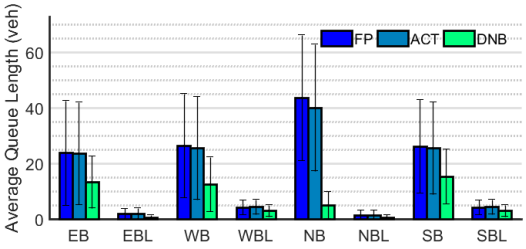

(b) Average queue length at 1.2 flow ratio.

Figure 10: Average queue length vs. flow ratio.

intervals and different threat point values to study the effect of these parameters on the controller's performance. The experimental results using the DNB controller show that, using relatively short updating time intervals, it is possible to minimize delay and maximize traffic flow efficiency. To evaluate the benefits of using the proposed controller, three scenarios were simulated using the three control approaches for different traffic demand levels. The results showed significant reductions in the average total delay ranging from 41% to 64%, a reduction in the average queue length ranging from 58% to 77%, a reduction in the emission levels ranging from 6% to 17%, a reduction in the average travel time ranging from 37% to 65%, and a reduction in the network clearance time ranging from 1% to 12%. To further investigate the achieved improvements using the DNB controller, simulations were conducted at different flow ratios. The simulation results demonstrated a significant potential for the DNB controller over FP and ACT controllers. Moreover, the results showed that major improvements were achievable using the DNB controller regardless of the traffic demand level. The next section integrates the developed DNB controller with transit signal priority (TSP) and freight signal priority (FSP) to maximize flows in real-time.

5 Signal Priority (SP)

This section integrates the developed DNB controller with TSP and FSP to maximize flows in real-time using high-fidelity data collected from vehicles through vehicle-to-infrastructure (V2I) wireless communication. V2I communication allows traffic signal controllers to dynamically respond to real-time traffic conditions to reduce the network delay and maximize traffic throughput. Experiments were conducted using the DNB controller on an intersection (Figure 5), with the traffic demand shown in Table 4.

Traffic signal priority was integrated in the developed DNB controller (DNB-SP), through a length-based (LB) passenger car equivalency, and formulated mathematically as (only Equation 3 is updated in the controller's formulation) shown below, where q_l^t is the number of queued vehicles in lane l at time t.

$$q_l^t = \sum_{v \in v_l^t} q_v^t \tag{8}$$

$$q_v^t = \begin{cases} \text{LB} & \text{if } s_v^{t-1} > s^{Th} \;\&\; s_v^t \leq s^{Th} \\ -\text{LB} & \text{if } s_v^{t-1} \leq s^{Th} \;\&\; s_v^t > s^{Th} \\ 0 & \begin{cases} \text{if } s_v^{t-1} \leq s^{Th} \;\&\; s_v^t \leq s^{Th} \\ \text{if } s_v^{t-1} > s^{Th} \;\&\; s_v^t > s^{Th} \end{cases} \end{cases} \tag{9}$$

The performance of the DNB-SP controller was compared to the DNB controller and a decentralized PSC controller to evaluate the performance of the proposed decentralized controller.

5.1 Transit Signal Priority (TSP)

This section presents the results of incorporating TSP logic within the DNB controller. TSP facilitates the movement of in-service transit vehicles through traffic-signal controlled intersections, and the TSP decisions are granted locally by the intersection controller.

The simulations were conducted using the following parameter values: 4525 passenger vehicles (PVs; 97% of the total demand), 146 buses (3% of the total demand), bus length equivalency of 3 passenger cars (LB = 3), and bus occupancy of 30 passengers (this parameter is used to compute the passenger travel time). Table 7 shows the average MOEs using PSC and DNB controllers for passenger vehicles and buses.

Table 8 shows the average MOEs using the DNB-SP controller for PVs and buses. The simulation results show that the DNB-SP controller produced major improvements for both the PVs and the buses in all MOEs.

Table 7: Average MOEs Using PSC & DNB Controller for PVs and Buses

MOE \ System	PSC			DNB		
	PV	Bus	Average	PV	Bus	Average
Average Vehicle Travel Time (s)	323.76	329.69	323.95	94.35	105.53	94.70
Average Passenger Travel Time (s)	323.76	330.54	327.19	94.35	106.89	100.53
Average Total Delay (s/veh)	104.94	107.13	105.01	51.50	61.66	51.82
Average Stopped Delay (s/veh)	64.34	59.05	64.17	20.21	23.79	20.32
Average Fuel (L)	0.13	0.21	0.14	0.12	0.18	0.12
Average CO_2 (grams)	288.76	554.03	297.05	245.38	464.91	252.24

Table 8: Average MOEs Using DNB-SP Controller for PVs and Buses

MOE \ System	DNB-SP		
	PV	Bus	Average
Average Vehicle Travel Time (s)	72.55	77.95	72.72
Average Passenger Travel Time (s)	72.55	79.08	75.77
Average Total Delay (s/veh)	45.39	50.25	45.55
Average Stopped Delay (s/veh)	17.62	13.96	17.50
Average Fuel (L)	0.11	0.17	0.12
Average CO_2 (grams)	238.04	449.66	244.65

In addition, Table 9 shows the percent improvement in MOEs for different vehicle classes using the proposed DNB-SP controller relative to the PSC and DNB controllers. Simulation results indicated significant improvements in various MOEs using the DNB-SP controller. Specifically, the average vehicle travel time decreased by 77.5%, the average passenger travel time decreased by 76.8%, the average total delay decreased by 56.6%, the average stopped delay decreased by 72.7%, and the fuel consumption decreased by 14.5% relative to the PSC controller. Moreover, the results demonstrated that the DNB-SP controller produced improvements in system performance relative to the DNB controller. Specifically, the DNB-SP controller produced reductions in the average vehicle travel time of 23%, the average passenger travel time of 24.6%, the average total delay of 12%, the average stopped delay of 13.8%, and the fuel consumption of 2.7%.

Table 9: TSP Improvement (%) Using DNB-SP Over PSC & DNB Controller

Improvement / MOE	DNB-SP over PSC (%)			DNB-SP over DNB (%)		
	PV	Bus	Average	PV	Bus	Average
Average Vehicle Travel Time (s)	77.59	76.36	77.55	23.11	26.14	23.21
Average Passenger Travel Time (s)	77.59	76.08	76.84	23.11	26.02	24.63
Average Total Delay (s/veh)	56.74	53.09	56.63	11.86	18.50	12.11
Average Stopped Delay (s/veh)	56.74	53.09	56.63	12.83	41.32	13.87
Average Fuel (L)	14.30	18.98	14.49	2.72	3.35	2.68
Average CO_2 (grams)	17.56	18.84	17.64	2.99	3.28	3.01

The results showed that the DNB-SP controller yielded significant improvements in the MOE values for different vehicle classes, indicating improved system efficiency.

5.2 Freight Signal Priority (FSP)

This section presents the results of integrating the FSP in the DNB controller. The simulations were conducted using the following parameter values: 4525 PVs (97% of total demand), 146 trucks (3% of total demand), truck length equivalency of 5 passenger cars (LB=5), and truck occupancy of 1 passenger. Table 10 shows the average MOEs using PSC and DNB controllers for PVs and trucks.

Table 10: Average MOEs Using PSC & DNB Controller for PVs and Trucks

System / MOE	PSC			DNB		
	PV	Truck	Average	PV	Truck	Average
Average Vehicle Travel Time (s)	513.38	533.89	514.02	178.61	193.17	179.06
Average Passenger Travel Time (s)	513.38	533.89	514.02	178.61	193.17	179.06
Average Total Delay (s/veh)	111.86	127.37	112.35	55.75	75.43	56.37
Average Stopped Delay (s/veh)	68.46	70.34	68.51	22.18	28.33	22.37
Average Fuel (L)	0.14	0.20	0.14	0.12	0.16	0.12
Average CO_2 (grams)	296.36	520.79	303.38	249.08	427.81	254.67

Table 11 shows the average MOEs using DNB-SP controller for passenger vehicles (PV) and trucks.

The simulation results showed that the DNB-SP controller exhibited major improvements for both the PVs and the trucks in all MOEs.

Table 11: Average MOEs Using DNB-SP Controller for PVs and Trucks

System / MOE	DNB-SP		
	PV	Truck	Average
Average Vehicle Travel Time (s)	108.50	120.59	108.88
Average Passenger Travel Time (s)	108.50	120.59	108.88
Average Total Delay (s/veh)	55.60	64.68	55.88
Average Stopped Delay (s/veh)	21.26	15.47	21.08
Average Fuel (L)	0.12	0.16	0.12
Average CO_2 (grams)	249.59	414.77	254.76

In addition, Table 12 shows the percent improvement in MOEs for different vehicle classes using the proposed DNB-SP controller over the PSC and DNB controllers. Simulation results indicated significant reductions in the average vehicle travel time of 78.8%, the average total delay of 50%, the average stopped delay of 69%, and fuel consumption of 13.3% relative to the PSC controller. Moreover, the results of using the DNB-SP controller showed reductions over the DNB controller in the average vehicle travel time of 39.2% and the average passenger travel time of 39.2%. Furthermore, the results showed an improvement for trucks in the average total delay of 14.2%, the average stopped delay of 45.4%, and the fuel consumption of 3% without or with slight impacts on the passenger vehicles.

The results showed that the DNB-SP controller yielded significant improvements in the average values of all MOEs for different vehicle classes. The next section entails extending the work to test the DNB controller on an arterial network of multiple intersections.

Table 12: FSP Improvement (%) Using DNB-SP over PSC & DNB Controller

Improvement / MOE	DNB-SP over PSC (%)			DNB-SP over DNB (%)		
	PV	Truck	Average	PV	Truck	Average
Average Vehicle Travel Time (s)	78.87	77.41	78.82	39.25	37.57	39.20
Average Passenger Travel Time (s)	78.87	77.41	78.82	39.25	37.57	39.20
Average Total Delay (s/veh)	50.30	49.22	50.26	0.27	14.26	0.86
Average Stopped Delay (s/veh)	68.95	78.00	69.24	4.16	45.39	5.80
Average Fuel (L)	12.98	20.51	13.31	-0.25	3.07	-0.08
Average CO_2 (grams)	15.78	20.36	16.03	-0.21	3.05	-0.04

6 Arterial Network Results

This section describes the testing of the proposed decentralized DNB controller, considering a variable phasing sequence and free cycle length on an arterial network.

6.1 Experimental Setup

The proposed controller was simulated on an arterial network located in the heart of downtown of Blacksburg, shown in Figure 11. The O-D demand matrices were generated using QueensOD software [81], and were based on counts collected during the afternoon peak period ($4-6$ PM), at 15 minute intervals, for the year 2012, [82].

A three-phase signalized intersection scheme (Figure 12) was used to represent the intersection phases applied in the downtown Blacksburg network, with protected leading main street left-turn phases [79]. The three phases represent the three players ($\mathrm{N}=3$) in the game.

The performance of the DNB controller was compared to the operation of an optimum FP controller, a centralized adaptive PS controller, a PSC controller [4], and a fully coordinated adaptive PSCO controller [23, 24] to evaluate its performance.

The simulations were conducted using the following parameter values: free-flow speed (40 km/h) based on the roadway speed limit, speed-at-capacity (29 km/h), jam density (160 veh/km/lane), saturation flow rate (1800 veh/h/lane), threshold speed (s^{Th}=4.5 km/h). These values were based on field measurements and typical values for arterial roadways. The FP was simulated using the observed signals' times in the field.

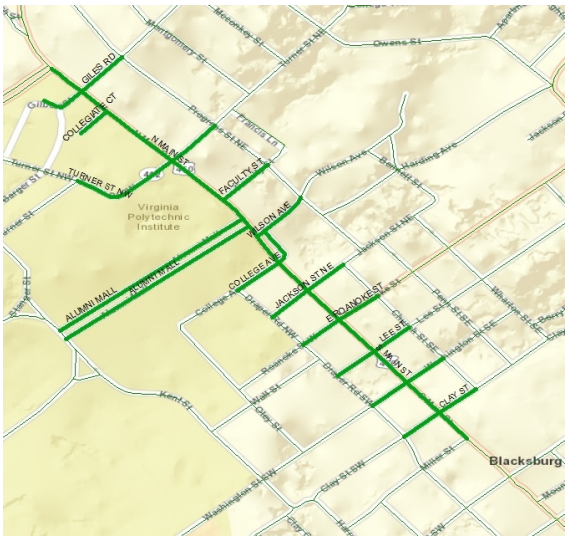

(a) Google image.

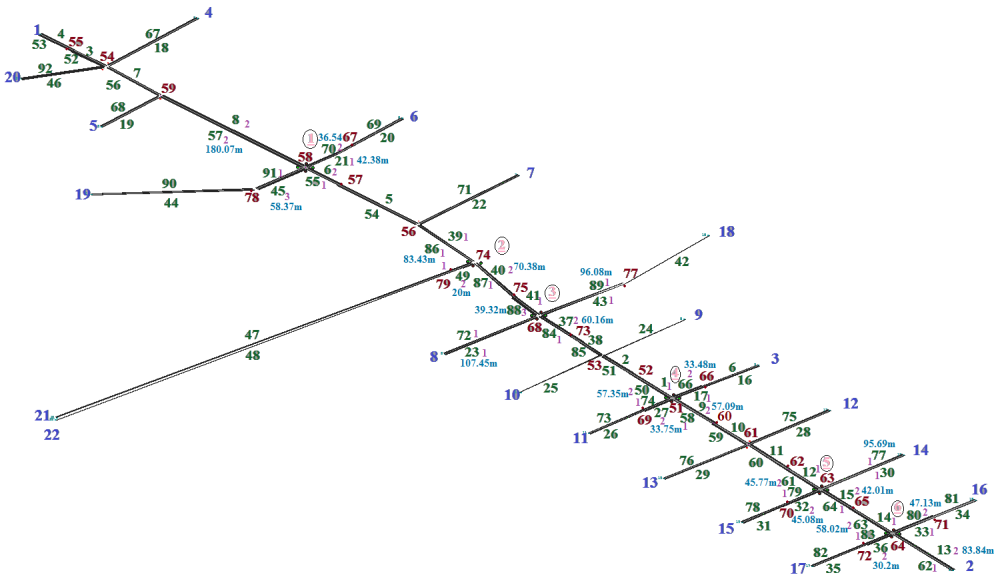

(b) INTEGRATION model.

Figure 11: Blacksburg testbed arterial network.

PS was optimized every 120 s. PSC and PSCO were optimized every 120 s, considering a minimum cycle length of 30 s and a maximum cycle length of 120 s. In the simulation, vehicles were allowed to enter the links in the first 2 hours, and the simulation ran for an extra 15 minutes to guarantee that all vehicles exited the network.

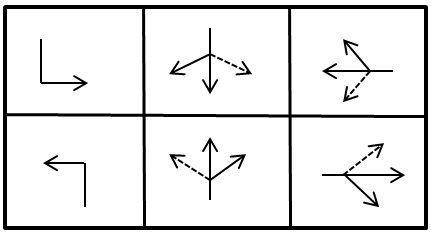

Figure 12: Phasing scheme.

6.2 Experimental Results

The simulation results shown below represent the average of 30 simulation runs at random seeds. The performance of the arterial network using the DNB controller was conducted such that the threat points were chosen based on the number of vehicles that each phase could accommodate based on the link lengths and number of lanes considering an updating time interval of 10 s.

Figure 13 shows the average values and the standard deviations of the MOEs across all movements over the entire simulation time for each control system, (FP, PS, PSC, PSCO, and DNB). The DNB controller outperformed other control approaches for all movements with a significant reduction in both the average values and the standard deviations for the total delay, stopped delay, travel time, fuel consumption, and CO_2 emissions.

In addition, Table 13 shows the percent improvement in MOEs using the proposed DNB approach over other approaches for 30 simulations with random seeds. Analysis of the results in Table 13 demonstrated the following: the proposed DNB approach outperformed other approaches in terms of average total delay, average travel time, average fuel consumed, average CO_2 emitted, and the clearance time of the last vehicle.

Figure 14 shows the average queue length for the six intersections, across all movements. The DNB control system outperformed other control systems (FP, PS, PSC, PSCO) for all movements. The simulation results showed that the DNB controller exhibited major improvements in the average values and the standard deviations of all MOEs for different movements, indicating that the system's efficiency was improved.

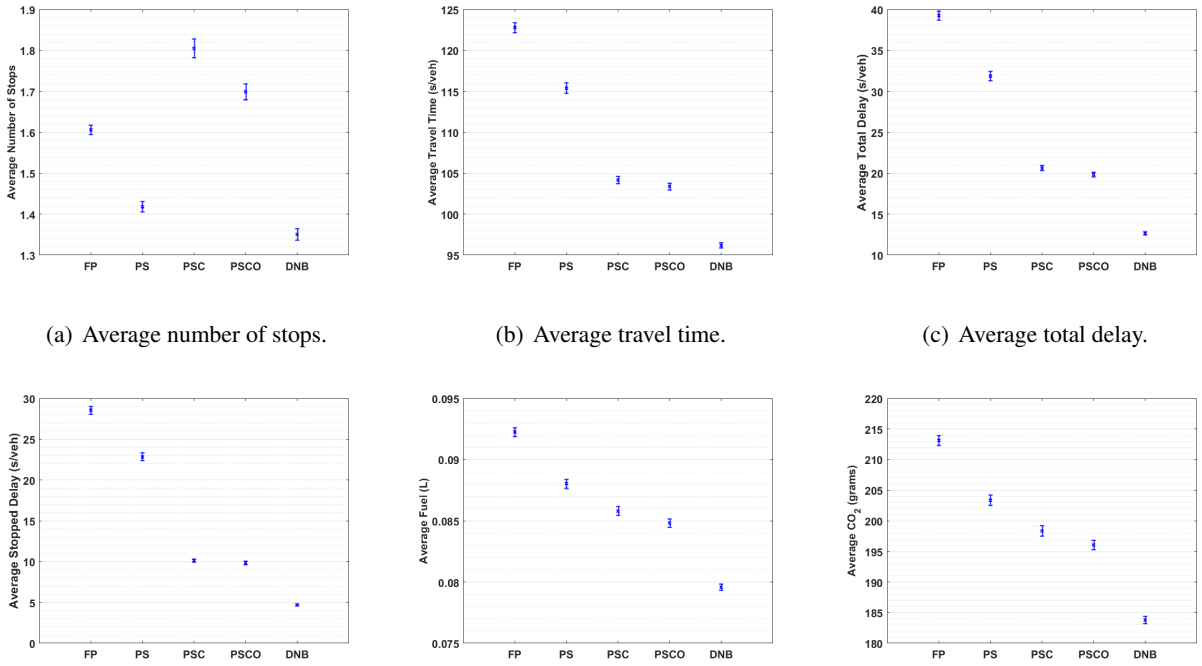

(a) Average number of stops. (b) Average travel time. (c) Average total delay.

(d) Average stopped delay. (e) Average fuel. (f) Average CO_2.

Figure 13: Average MOEs of 30 simulations at random seeds.

Table 13: Average MOEs and the Percent Improvement Using DNB Controller over Other Controllers

MOE \ System	FP	PS	PSC	PSCO	DNB
Average Total Delay (s/veh)	39.255	31.847	20.609	19.833	12.649
Improvement %	67.777	60.282	38.624	36.223	
Average Stopped Delay (s/veh)	28.549	22.849	10.127	9.849	4.686
Improvement %	83.585	79.490	53.723	52.418	
Average Travel time (s)	122.780	115.376	104.155	103.373	96.188
Improvement %	21.658	16.630	7.649	6.950	
Average Number of Stops	1.605	1.418	1.805	1.699	1.350
Improvement %	15.879	4.776	25.205	20.522	
Average Fuel (L)	0.092	0.088	0.086	0.085	0.080
Improvement %	13.740	9.617	7.256	6.170	
Average CO2 (grams)	213.114	203.352	198.322	196.003	183.820
Improvement %	13.746	9.605	7.312	6.216	
Last Vehicle Arrival time (s)	7380.9	7328.0	7316.8	7338.9	7311.9
Improvement %	0.935	0.220	0.067	0.368	

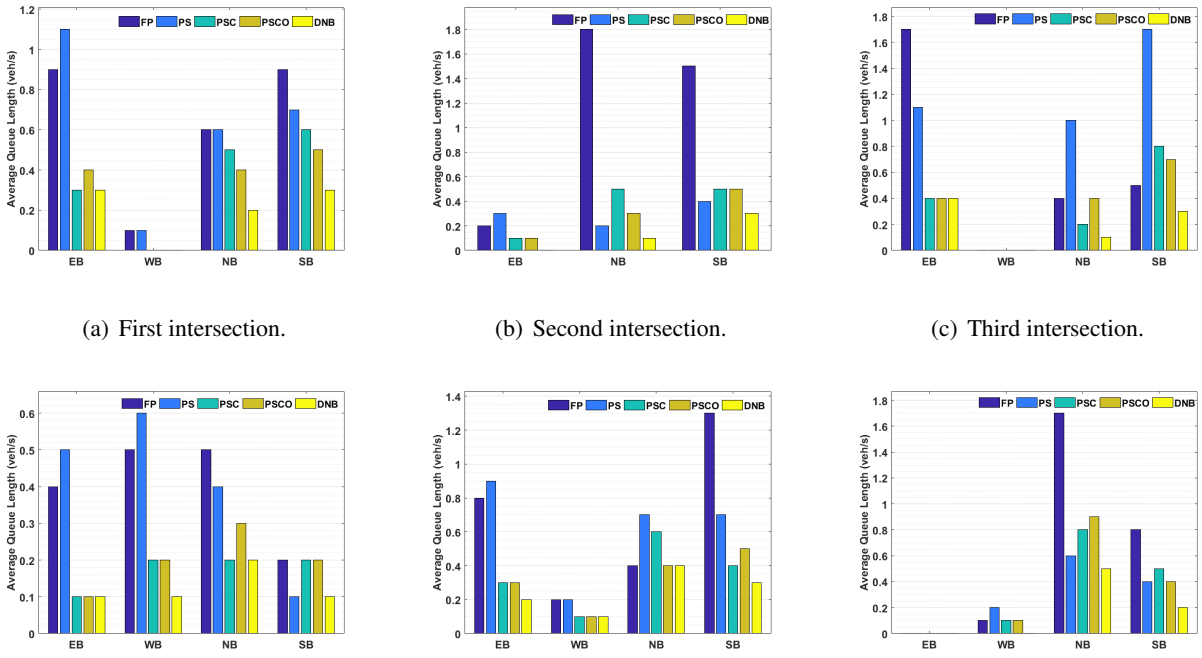

(a) First intersection. (b) Second intersection. (c) Third intersection.

(d) Fourth intersection. (e) Fifth intersection. (f) Sixth intersection.

Figure 14: Average queue length of the intersections.

6.3 Statistical Analysis

To study the statistical significance of these findings, we applied an analysis of variance (ANOVA) test to the data. ANOVA is a statistical test used to identify significant differences between the means of three or more independent groups. The ANOVA test was applied to all MOEs; however, only the results for the average total delay are shown here.

Figure 15 shows that the assumptions of the ANOVA test were validated; i.e., the results show normality and equal variance. The distribution of the studentized residuals follow a normal distribution, and have equal variances. Table 14 shows that the null hypothesis for ANOVA—i.e., the mean is the same for all approaches—is rejected, and at least one approach, has a statistically significant different mean.

In addition, we applied the Tukey test to determine which approaches were similar. Table 15 shows the results of the Tukey test, where levels not connected by the same letter are significantly different.

Moreover, a pairwise comparison test was conducted to compare approaches in pairs to identify the approaches with similar MOEs. The results shown in Table 16 conclude that the DNB control approach exhibited major, statistically significant improvements over other approaches.

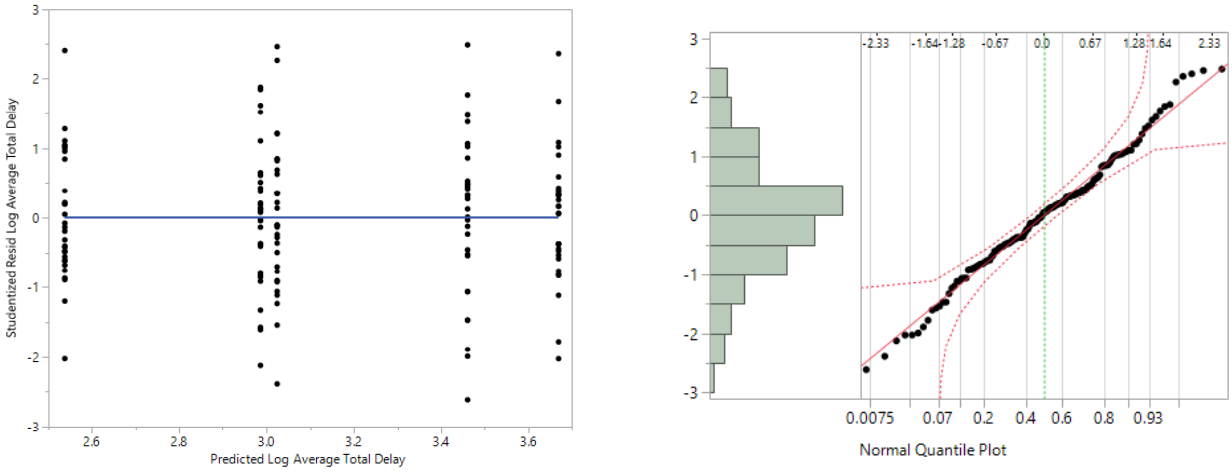

(a) Variance.

(b) Normality.

Figure 15: Assumptions of ANOVA test.

Table 14: Analysis of Variance

Source	DF	Sum of Squares	Mean Square	F Ratio	Prob>F
Algorithm	4	23.492544	5.87314	25124.81	<0.0001
Error	145	0.033895	0.00023		
C. Total	149	23.526439			

Table 15: Tukey Test

Level		Least Square Mean
FP	A	3.6699004
PS	B	3.4607800
PSC	C	3.0255877
PSCO	D	2.9872279
DNB	E	2.5374774

6.4 Summary

In this section the developed DNB decentralized cycle-free traffic signal controller was applied on an arterial network. INTEGRATION microscopic traffic assignment and simulation software was used to evaluate the

Table 16: Pairwise Comparison

Level	-Level	Difference	Std Err Dif	Lower CL	Upper CL	P-Value
FP	DNB	1.132423	0.0039476	1.121518	1.143328	<0.0001
PS	DNB	0.923303	0.0039476	0.912398	0.934208	<0.0001
FP	PSCO	0.682672	0.0039476	0.671767	0.693577	<0.0001
FP	PSC	0.644313	0.0039476	0.633408	0.655218	<0.0001
PSC	DNB	0.488110	0.0039476	0.477205	0.499015	<0.0001
PS	PSCO	0.473552	0.0039476	0.462647	0.484457	<0.0001
PSCO	DNB	0.449750	0.0039476	0.438845	0.460655	<0.0001
PS	PSC	0.435192	0.0039476	0.424287	0.446097	<0.0001
FP	PS	0.209120	0.0039476	0.198215	0.220025	<0.0001
PSC	PSCO	0.038360	0.0039476	0.027455	0.049265	<0.0001

performance of the proposed controller relative to the operation of an optimum FP controller, a centralized adaptive PS controller, a PSC controller [4], and a fully coordinated adaptive PSCO controller, on an arterial network in downtown Blacksburg, VA. A total of 30 random seed simulations were conducted for the five control approaches. The experimental results using the DNB controller showed that, with a flexible phasing sequence and free cycle length control strategy, it was possible to minimize delay and maximize traffic flow efficiency. The results showed significant reductions in the average queue length, in the average total delay ranging from 36% to 67%, in the emission levels ranging from 6% to 13%, in the average travel time ranging from 7% to 21%, and in the network clearance time.

ANOVA tests, Tukey tests, and pairwise comparison tests were conducted to validate the benefits of using the proposed DNB control approach, and the results showed that the DNB controller produced major improvements over other approaches. The results demonstrated a significant potential for the proposed controller over other state-of-the-art centralized and decentralized control approaches. The next section entails extending the work to test the DNB controller on large scale networks.

7 Large-Scale Network & Sensitivity Analysis

This section describes the application and testing of the proposed decentralized cycle-free DNB controller on large-scale networks. The developed controller was compared to the operation of a decentralized PSC controller and a fully coordinated adaptive PSCO controller to evaluate its performance [83]. The section is organized as follows. Section 7.1 presents the experimental setup and results of large scale studies in the town of Blacksburg, VA, consisting of 38 signalized intersections. Section 7.2 describes the experimental setup and the experimental results of large scale studies on a downtown network in Los Angeles, CA, consisting of 457 signalized intersections.

7.1 Blacksburg Town Experiments

7.1.1 Blacksburg Experimental Setup

These experiments were large scale studies carried out in the town of Blacksburg, VA, shown in Figure 16. The simulations were conducted using the morning peak hour (7–8 a.m.) traffic demand. The town of Blacksburg has 38 signalized intersections, 549 stop signs, 30 yield signs, and 1,844 links.

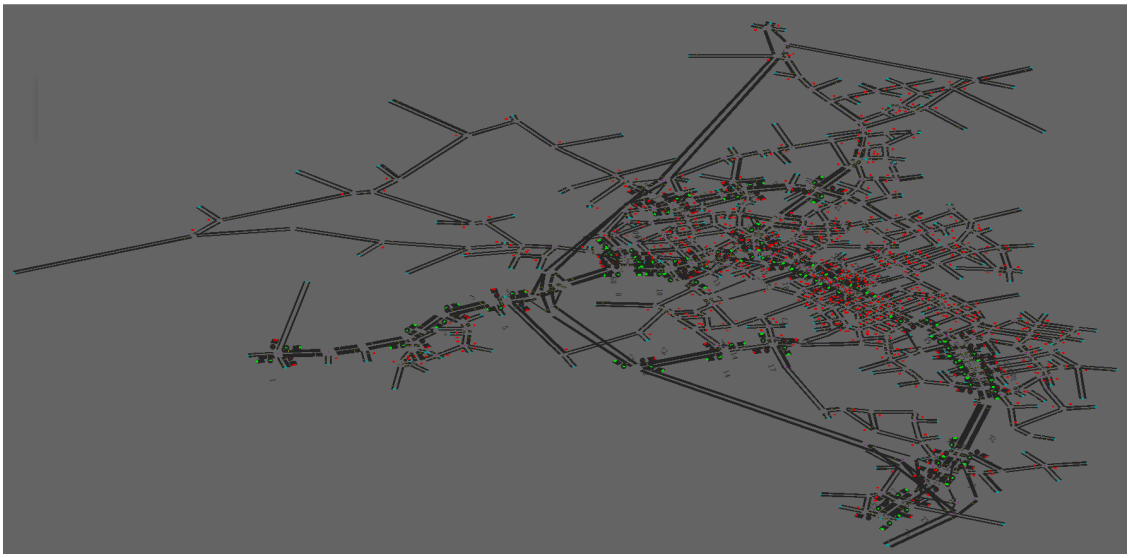

Figure 16: Blacksburg network.

The O-D demand matrices were generated using the QueensOD software [81] and consisted of 23,260 trips. The phasing scheme varied between 2 to 4 phases, reflecting the intersection phases implemented in the town. The minimum free-flow speed on the network was 30 (km/h), and the maximum free-flow speed

on the network was $105\ (\mathrm{km/h})$. The minimum link length on the network was $50\ \mathrm{m}$, and the maximum link length on the network was $2,932\ \mathrm{m}$. The jam density on the network was equal to $160\ (\mathrm{veh/km/lane})$. The performance of the DNB controller was compared to the operation of PSC and PSCO controllers to serve as a reference for the evaluation of the proposed decentralized controller's performance. The average of each of the following MOEs was calculated to assess the DNB controller's performance: total delay, travel time, stopped delay, queue length, fuel consumption, and emission levels. In the simulations, vehicles could enter the links for an hour, and the simulation ran for an extra time past that hour to guarantee that all vehicles departed the network. INTEGRATION microscopic traffic simulation software was used to model the network, shown in Figure 16. Two experiments were conducted on the Blacksburg network, as discussed in the following sections.

7.1.2 First Experimental Results (Blacksburg)

In this experiment, the performance of the DNB controller was compared to PSC and PSCO controllers. The threat point (d) values per lane for the DNB controller were assigned based on the link's lengths (L), the link's free-flow speeds ($\mathrm{U_f}$), and the updating time intervals ($\Delta\mathrm{t}$) using the following formula: d=min[$\mathrm{N(L/2)}$, $\mathrm{N(U_f \times \Delta t)}$], where $\mathrm{N(L/2)}$ represents the number of vehicles that could be accumulated up to the half length of the link, and $\mathrm{N(U_f \times \Delta t)}$ represents the number of vehicles that could be accumulated up to the distance of ($\mathrm{U_f \times \Delta t}$). Using the distance of $\mathrm{U_f \times \Delta t}$ allowed detected vehicles to pass the intersection without stopping if there was no queue in front of them, where $\mathrm{L/2}$ was used instead of L to get a better estimate of the queue length for each movement, as drivers generally move to the appropriate lanes as approaching the signalized intersection, and to avoid being fully queued (i.e., players will accept a fully occupied [queued] link).

The average MOEs values over the entire simulation time for the PSC, PSCO and DNB controllers are shown in Table 17. In addition, Table 17 shows the percent improvement in MOEs when using the proposed DNB controller versus PSC and PSCO controllers.

Simulation results indicated significant reduction in the average total delay of 16.5%, a reduction in the average stopped delay of 40.3%, and a reduction in the average travel time of 5.25%, over the PSC controller. In addition, the results indicated significant reduction in the average total delay of 19.8%, a reduction in the average stopped delay of 52.7%, and a reduction in the average travel time of 6.5%, over the PSCO controller. These results show that the proposed DNB controller outperformed both PSC and PSCO controllers.

Table 17: Average MOEs and (%) Improvement Using DNB over PSC and PSCO Controllers

MOE \ System	PSC	PSCO	DNB
Average Total Delay (s/veh)	96.234	100.197	80.323
Improvement %	16.534	19.823	
Average Stopped Delay (s/veh)	20.285	25.649	12.1074
Improvement %	40.314	52.7962	
Average Travel time (s)	306.254	310.225	290.175
Improvement %	5.250	6.463	
Average Number of Stops	4.662	4.5899	4.281
Improvement %	8.18	6.734	
Average Fuel (L)	0.4142	0.4129	0.40
Improvement %	3.38	3.07	
Average CO2 (grams)	913.833	912.495	883.127
Improvement %	3.36	3.22	

7.1.3 Second Experimental Results (Blacksburg)

The minimum free-flow speed on the network was $30\ (\mathrm{km/h})$, and the maximum free-flow speed on the network was $105\ (\mathrm{km/h})$, with updating time intervals of $10\ \mathrm{s}$. Assigning the detectors' locations to be the min($\mathrm{L}/2$, $\mathrm{U_f} \times \Delta\mathrm{t}$), the detectors could be located for long links between $84\ \mathrm{m}\ (\mathrm{i.e.}, 13\ \mathrm{veh/lane})$ to $292\ \mathrm{m}\ (\mathrm{i.e.}, 47\ \mathrm{veh/lane})$, employing the free-flow speed to determine the disagreement point.

(d=min[$\mathrm{N}(\mathrm{L}/2)$, $\mathrm{N}(\mathrm{U_f} \times \Delta\mathrm{t})$]) is a good choice for low traffic demand, as vehicles are not to stop at the intersection); however, for high traffic demand, long links can accommodate long queues, which causes delays for the vehicles on that link.

Hence, reducing the number of vehicles that can accumulate in a lane might enhance the network's performance. To examine the effectiveness of improving the MOEs by changing the maximum number of vehicles that could be accumulated per lane, a sensitivity analysis was conducted, as shown in Figure 17, with d=min[$\mathrm{N}(\mathrm{L}/2)$, NV], where NV represents the maximum number of vehicles that can accumulate in a lane; this number ranges between 6 and 32 vehicles.

Analysis of the results in Figure 17 demonstrates that better performance could be achieved using the DNB controller by assigning the threat point as a minimum of 12 veh/lane and the number of vehicles that could be accumulated as $\mathrm{L}/2$, (d=min[$\mathrm{N}(\mathrm{L}/2)$, 12]).

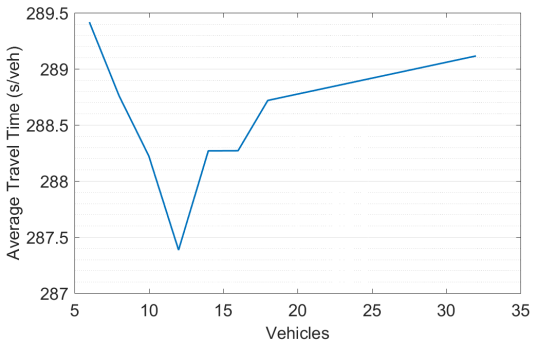

(a) Average travel time.

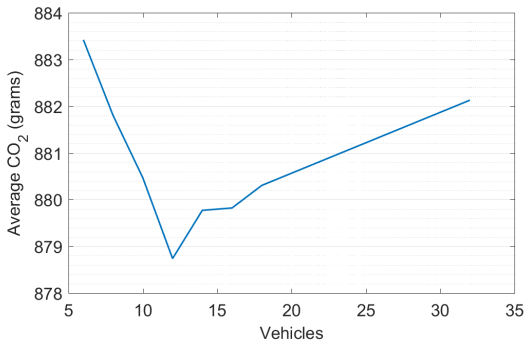

(b) Average CO_2.

Figure 17: Sensitivity analysis.

Table 18 shows the average MOEs values over the entire simulation time and the percent improvement in MOEs using the proposed DNB controller over PSC and PSCO controllers.

Simulation results indicate significant reduction in the average total delay of 19.38%, a reduction in the average stopped delay of 51.18%, a reduction in the average travel time of 6.162%, a reduction in the average number of stops of 8.39%, a reduction in the average fuel consumption of 3.89%, and a reduction in the emission levels of 3.84%, over the PSC controller. The results show that the proposed DNB controller outperformed both the PSC and PSCO controllers.

Table 18: Average MOEs and (%) Improvement Using DNB over PSC & PSCO Controllers

System / **MOE**	PSC	PSCO	DNB
Average Total Delay (s/veh)	96.234	100.197	77.577
Improvement %	19.3871	22.575	
Average Stopped Delay (s/veh)	20.285	25.649	9.903
Improvement %	51.182	61.391	
Average Travel Time (s)	306.254	310.225	287.384
Improvement %	6.162	7.362	
Average Number of Stops	4.662	4.5899	4.271
Improvement %	8.393	6.95	
Average Fuel (L)	0.4142	0.4129	0.3981
Improvement %	3.887	3.584	
Average CO2 (grams)	913.833	912.495	878.739
Improvement %	3.84	3.7	

To further investigate the achieved improvements using the DNB controller, it was taken into consideration that the network has 459 stop signs and 30 yield signs, which might conceal the full degree of improvement achieved using the DNB controller on the signalized intersection. Accordingly, we investigated the percent improvement in MOEs using the DNB controller versus the PSC controller over only the links that were directly associated with intersections. Table 19 shows the percent improvement in MOEs using the DNB controller over the PSC controller on the 38 intersections. Table 19 demonstrates an improvement in the travel time on the intersections between 6% to 52%, an improvement in the queue length on the intersections between 8% to 60%, and an improvement in the number of stops on the intersections between 8% to 80%. In addition, Table 19 demonstrates an overall reduction in the average travel time of 23.63%, in the average queued vehicles of 37.66%, in the average number of stops of 23.58%, in the average fuel consumption of 10.44%, in the average CO_2 emitted of 9.84%, and in the average NO_x emitted of 5.4% over the PSC controller. These results reveal that the DNB controller performed significantly better than the PSC controller.

Table 19: Intersections (%) Improvement of MOEs Using DNB over PSC Controller

MOEs / Int. #	Travel Time	Queue	Num. of Stops	CO_2	Fuel	NO_x
1	6.153	22.015	24.311	2.645	2.566	0.161
2	16.409	26.801	21.184	7.706	7.710	5.859
3	8.485	18.233	32.777	6.034	6.450	9.040
4	31.114	52.874	39.564	8.166	6.595	8.756
5	22.230	53.875	52.914	9.355	8.962	3.309
6	23.176	34.435	14.240	11.594	10.716	4.751
7	8.967	15.881	17.832	3.889	3.597	2.271
8	24.057	41.868	16.114	13.753	13.480	9.162
9	40.709	56.267	29.850	25.253	24.654	13.842
10	13.395	26.346	41.436	8.634	8.653	9.772
11	17.628	26.340	11.802	9.014	8.353	1.352
12	7.642	7.968	32.650	3.481	3.373	3.476
13	19.414	37.909	20.915	8.991	8.745	3.758
14	28.503	35.499	25.359	7.854	6.617	8.147
15	23.870	39.630	34.584	12.553	12.272	6.166
16	27.552	59.095	41.876	15.109	14.785	8.836
17	42.001	60.000	56.974	16.896	14.827	12.842
18	26.258	49.883	32.723	14.491	13.414	5.703
19	19.676	36.533	21.104	4.963	4.253	4.976
20	52.237	76.083	63.088	32.966	31.762	20.159
21	34.822	50.159	46.265	21.568	21.385	18.268
22	38.267	59.396	37.466	27.628	27.284	26.528
23	17.193	30.863	16.272	7.595	6.922	5.258
24	34.669	43.997	11.269	14.632	13.342	3.239
25	23.480	44.588	57.381	5.760	4.502	0.085
26	18.029	26.028	30.503	4.017	2.478	0.750
27	28.129	36.340	8.565	16.769	16.194	14.480
28	14.530	35.046	11.902	9.459	9.846	11.611
29	13.131	19.115	9.603	5.347	4.985	1.142
30	23.632	47.382	23.224	19.330	19.409	24.772
31	32.761	55.701	80.381	18.004	17.273	19.333
32	34.761	53.070	35.456	26.641	27.045	29.311
33	35.984	48.472	15.256	20.348	19.563	11.668
34	16.679	32.676	30.335	11.273	11.151	11.757
35	18.012	28.950	21.575	18.241	18.672	26.116
36	22.588	46.509	34.331	7.676	7.028	2.465
37	29.307	46.502	31.486	7.399	6.678	1.081
38	14.317	14.552	8.061	4.669	4.168	1.143
Overall (%)	23.633	37.666	23.586	10.444	9.842	5.390

7.2 Downtown Los Angeles Experiments

7.2.1 Los Angeles Experimental Setup

These experiments were large scale studies of a network in downtown Los Angeles, CA, including the most congested downtown area, as shown in Figure 18. Simulations were conducted during the morning peak hour ($7 - 8$ a.m.) [84]. The downtown Los Angeles network has 457 signalized intersections, 285 stop signs, 23 yield signs, and $3,556$ links. The O-D demand matrices were generated using the QueensOD software [81] with $143,957$ trips. The phasing scheme varied from 2 to 6 phases, reflecting the intersection phases implemented in downtown Los Angeles. The minimum free-flow speed on the network was 15 $(\mathrm{km/h})$, and the maximum free-flow speed on the network was 120 $(\mathrm{km/h})$. The minimum link length on the network was 50 m, and the maximum link length on the network was 4400 m. The jam density on the network was equal to 180 $(\mathrm{veh/km/lane})$.

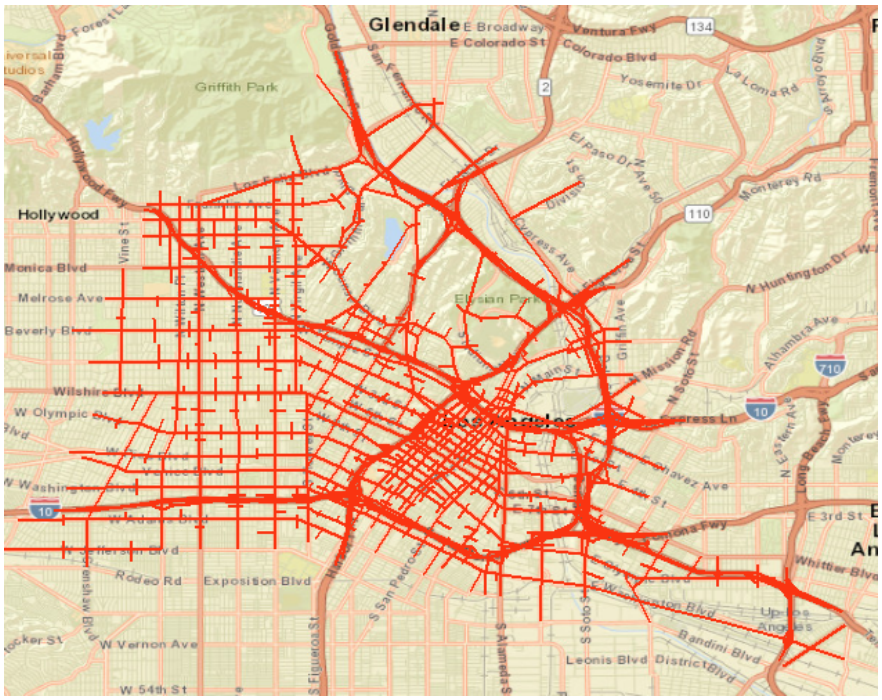

Figure 18: Downtown Los Angeles, Google maps.

The DNB controller was compared to the PSC controller to evaluate their relative performance. The average of each of the following MOEs was calculated to assess the performance of the DNB controller: total delay, travel time, stopped delay, queue length, fuel consumption, and emission levels. In the simulations, vehicles could enter the links for an hour, with extra time at the end of the simulation to guarantee that all

vehicles departed the network. INTEGRATION microscopic traffic simulation software was used to model the network, as shown in Figure 19.

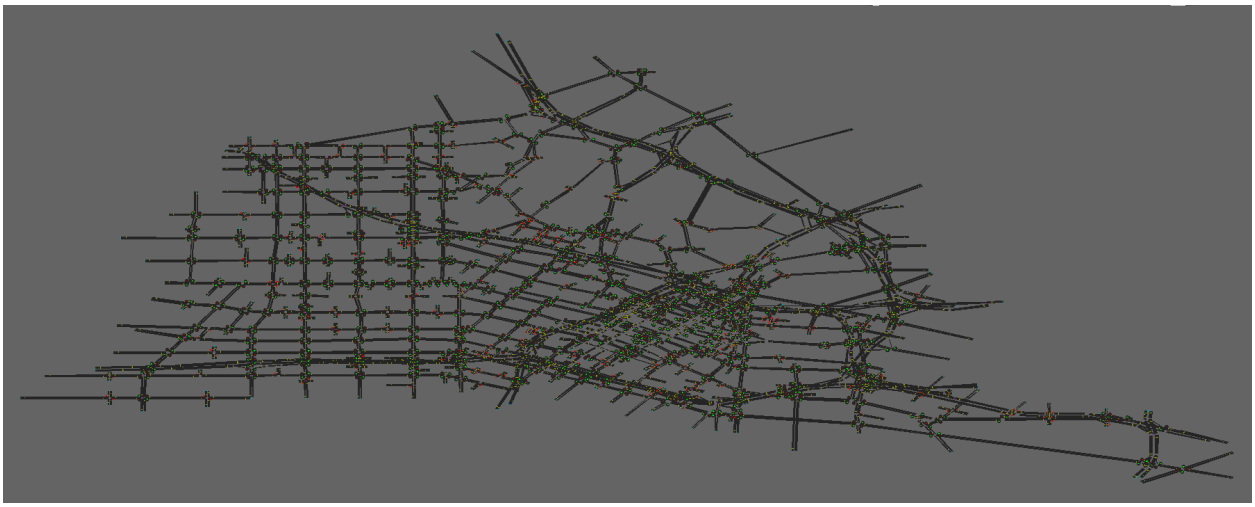

Figure 19: INTEGRATION, Los Angeles network.

7.2.2 First Experimental Results (Los Angeles)

In this experiment, the DNB controller's performance was compared to that of the PSC controller using the full demand in the morning peak hour. The threat point per lane for the DNB controller was assigned as the minimum of 12 veh/lane and the number of vehicles that could be accumulated on $L/2$ (i.e., d=min[$N(L/2)$, 12]) based on the sensitivity analysis shown in Figure 20.

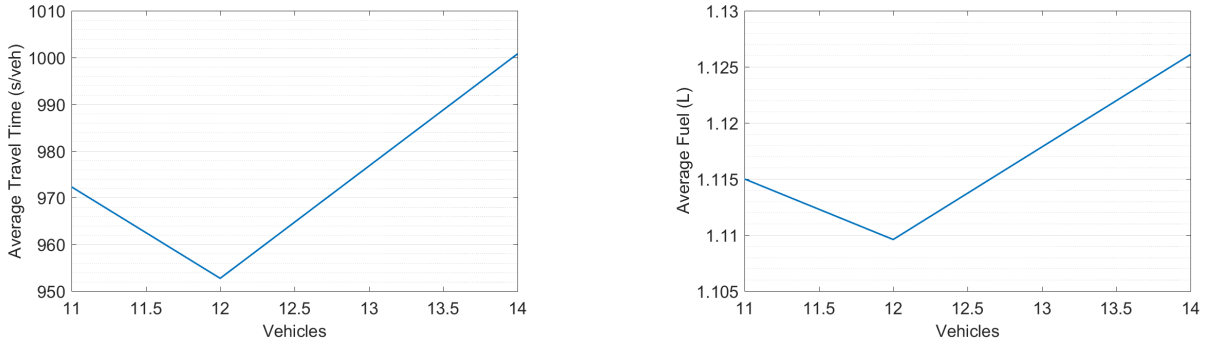

(a) Average Travel Time.

(b) Average Fuel Consumption.

Figure 20: Los Angeles sensitivity analysis.

The average MOEs values over the entire simulation time for PSC and DNB controllers are shown

in Table 20. In addition, Table 20 shows the percent improvement in MOEs using the proposed DNB controller over the PSC controller. Simulation results indicated significant reduction in the average total delay of 14.55%, a reduction in the average stopped delay of 25.18%, a reduction in the average travel time of 7.89%, a reduction in the average number of stops of 12.4%, a reduction in the average fuel consumption of 4.0%, and a reduction in the emission levels of 4.25%, for the DNB over the PSC controller. Analysis of the results demonstrates that the proposed DNB controller outperformed the PSC controller.

Table 20: Average MOEs and the (%) Improvement Using DNB Controller over PSC Controller (100% Demand)

System / **MOE**	PSC	DNB	DNB Imp. (%)
Average Total Delay (s/veh)	557.463	476.346	14.55
Average Stopped Delay (s/veh)	256.766	192.116	25.178
Average Travel Time (s)	1034.27	952.732	7.89
Average Number of Stops	7.406	6.487	12.4
Average Fuel (L)	1.155	1.109	4.0
Average CO_2 (grams)	2482.13	2376.59	4.25

To further investigate the achieved improvements using the DNB controller, it was taken into consideration that the network has 285 stop signs and 23 yield signs, which might conceal the full degree of improvement achieved using the DNB controller on the signalized intersection. Accordingly, we investigated the percent improvement in MOEs using the DNB controller over the PSC controller over only the links that were directly associated with intersections. Table 21 demonstrates a reduction in the average travel time of 35.16%, a reduction in the average queued vehicles of 54.67%, a reduction in the average number of stops of 44.03%, a reduction in the average fuel consumption of 9.97%, a reduction in the CO_2 emitted of 9.92%, and a reduction in the NO_x emitted of 11.78% over the PSC controller. These results reveal that the DNB controller has significantly better performance potential than the PSC controller.

7.2.3 Second Experimental Results (Los Angeles)

To further investigate performance potential using the DNB controller, a simulation was conducted at lower traffic conditions (i.e., 10% of the peak demand).

Table 22 shows a reduction in the average total delay of 36.79%, a reduction in the average stopped

Table 21: Average (%) Improvements of MOEs Using DNB Controller over PSC Controller (100% Demand), over the Links That Are Directly Associated with Intersections

MOEs / Int. #	Travel Time	Queue	Num. of Stops	CO_2	Fuel	NO_x
Overall 457 Int. (%)	35.156	54.669	44.031	9.966	9.919	11.774

delay of 90.26%, a reduction in the average travel time of 7.1%, a reduction in the average number of stops of 34.66%, a reduction in the average fuel consumption of 4.8%, and a reduction in the emission levels of 4.79%, over the PSC controller.

Table 22: Average MOEs and the (%) Improvement Using DNB over the PSC Controller (10% Demand)

System / MOE	PSC	DNB	DNB Imp. (%)
Average Total Delay (s/veh)	84.938	53.689	36.79
Average Stopped Delay (s/veh)	19.971	1.9451	90.261
Average Travel Time (s)	450.114	418.177	7.1
Average Number of Stops	4.475	2.924	34.66
Average Fuel (L)	0.846	0.805	4.8
Average CO_2 (grams)	1830.27	1742.53	4.79

Once more, To further investigate the achieved improvements using the DNB controller, it was taken into consideration that the network has 285 stop signs and 23 yield signs, which might conceal the full degree of improvement achieved using the DNB controller on the signalized intersection. Accordingly, we investigated the percent improvement in MOEs using the DNB controller versus the PSC controller over only the links that were directly associated with intersections at a lower demand, as shown in Table 23.

Table 23 demonstrates a reduction in the average travel time of 19.19%, a reduction in the average queued vehicles of 49.84%, a reduction in the average number of stops of 53.71%, a reduction in the average fuel consumption of 54.16%, a reduction in the average CO_2 emitted of 16.09%, and a reduction in the average NO_x emitted of 25.94% over PSC controller. These results reveal that the DNB controller performed significantly better than the PSC controller as the traffic demand decreased.

The results show that the DNB controller yielded significant improvements in the average values of all

Table 23: Average (%) Improvements of MOEs Using DNB over PSC Controller (10% Demand) over the Links Directly Associated with Intersections

MOEs / Int. #	Travel Time	Queue	Num. of Stops	CO_2	Fuel	NO_x
Overall 457 Int. (%)	19.186	49.844	53.708	54.158	16.085	25.939

MOEs, indicating improved system efficiency.

7.3 Summary

In this section, the developed DNB decentralized, cycle-free, flexible phasing traffic signal controller was applied and evaluated on large scale networks. INTEGRATION microscopic traffic assignment and simulation software was used to evaluate the performance of the proposed controller relative to a decentralized PSC optimization controller, and a fully-coordinated adaptive PSCO controller, in the town of Blacksburg, VA, and in downtown Los Angeles, CA.

Several simulations were conducted on the Blacksburg network using different threat point values to determine their effect on the controller's performance. The results showed significant reductions on the network in the average total delay of 19.3% and 22.6%, a reduction in the stopped delay of 51% and 61%, a reduction in the average travel time of 6.1% and 7.3%, and a reduction in the emission levels of 3.8% and 3.7%, over PSC and PSCO controllers, respectively. In addition, the results showed significant reductions on the intersections links in the average travel time of 23.6%, a reduction in the average queue length of 37.6%, a reduction in the average number of stops of 23.6%, a reduction in the Co_2 emitted of 10.4%, a reduction in the fuel consumption of 9.8%, and a reduction in NO_x emitted of 5.4%.

In addition, the DNB controller's performance was tested in downtown Los Angeles, CA, and compared to the performance of a PSC controller. The results showed significant reductions on the network in the average total delay of 14.5%, a reduction in the stopped delay of 25.1%, a reduction in the average travel time of 8%, a reduction in the average number of stops of 12.4% and a reduction in the Co_2 emitted of 4.25%, over the PSC controller. Moreover, the results showed significant reductions at the intersections links in the average travel time of 35.1%, a reduction in the average queue length of 54.7%, a reduction in the average number of stops of 44%, a reduction in the Co_2 emitted of 10%, a reduction in the fuel consumption of 10%, and a reduction in NO_x emitted of 11.7%. Furthermore, simulations conducted at

lower traffic flow conditions showed significant reductions on the network in the average total delay of 36.7%, a reduction in the stopped delay of 90.2%, and a reduction in the average number of stops of 35% over the PSC controller. As these results indicate, the DNB controller can generate major performance improvements at lower demands.

The results demonstrate significant potential benefits of using the proposed DNB controller over other state-of-the-art centralized and decentralized controllers on large scale networks.

8 Summary & Conclusions

Traffic growth constrained by available capacity in urban areas affects traveler mobility, air quality, and public health. Reducing traffic congestion can improve these conditions while simultaneously decreasing transportation-related energy use. To enhance air quality, optimizing the utilization of the available infrastructure via advanced traffic signal controllers is necessary to mitigate traffic congestion and emissions in a world with growing pressure on financial and physical resources. To mitigate traffic congestion at signalized intersections, we developed a novel real-time adaptive multi-modal decentralized traffic signal optimization controller, considering a flexible phasing sequence and free cycle length, using an NB game-theoretic framework (DNB controller).

The DNB controller is used to optimize the signal timings at each signalized intersection by modeling each phase as a player in a game, where players cooperate to reach a mutually agreeable outcome. Decentralized systems are scalable and easy to expand by inserting new controllers into the system. Additionally, decentralized systems are often inexpensive to establish and operate, as there is no essential need for a reliable and direct communication network between a central computer and the local controllers in the field. INTEGRATION microscopic traffic assignment and simulation software was used to evaluate the performance of the algorithm relative to an optimum FP and an ACT controller on a major intersection in downtown Toronto, considering different traffic demand levels, and using observed traffic data. Several simulations were conducted using the DNB controller with different update time intervals and different threat point values to study the effect of these parameters on the controller's performance. The experimental results using the DNB controller showed that, using a relatively short updating time interval, it was possible to minimize delay and maximize traffic flow efficiency. To evaluate the benefits of using the proposed controller, three scenarios were simulated using the three controllers at different traffic demand levels. The results showed significant reductions in the average total delay ranging from 41% to 64%, a reduction in the average queue length ranging from 58% to 77%, a reduction in the emission levels ranging from 6% to 17%, a reduction in the average travel time ranging from 37% to 65%, and a reduction in the network clearance time ranging from 1% to 12%. To further investigate the achieved improvements using the DNB controller, simulations were conducted at different flow ratios. The simulation results demonstrated a significant potential for the DNB controller over FP and ACT controllers. Moreover, the results showed that major improvements are achievable using the DNB controller regardless of the traffic demand level.

In addition, the proposed controller integrated TSP and FSP, to maximize flows in real-time using data

collected from vehicles through V2I wireless communications. The results of integrating the TSP in the developed controller on an isolated intersection showed an improvement in the average vehicle travel time of 77.5%, the average passenger travel time of 76.8%, the average total delay of 56.6%, the average stopped delay of 72.7%, the fuel consumption of 14.5%, and emissions of 17.6%. In addition, the results of integrating the FSP in the developed controller on an isolated intersection, showed an improvement in the average vehicle travel time of 78.8%, the average total delay of 50%, the average stopped delay of 69%, the fuel consumption of 13.3%, and emissions of 16%.

Furthermore, the proposed controller was applied on an arterial network in downtown Blacksburg, VA, which was composed of six intersections. INTEGRATION microscopic traffic assignment and simulation software was used to evaluate the performance of the proposed controller relative to an optimum FP controller, a centralized adaptive PS controller, a decentralized PSC controller, and a fully-coordinated adaptive PSCO controller. A total of 30 random seed simulations were conducted for the five controllers. The results showed significant reductions in the average queue length, in the average total delay ranging from 36% to 67%, a reduction in the emission levels ranging from 6% to 13%, a reduction in the average travel time ranging from 7% to 21%, and a reduction in the network clearance time. ANOVA, Tukey , and pairwise comparison tests were conducted to validate the benefits of using the proposed controller (DNB), and the results showed that the DNB controller produced statistically significant major improvements over other state-of-the-art centralized and decentralized control approaches.

Moreover, the developed DNB decentralized cycle-free with flexible phasing traffic signal controller was applied and evaluated on large scale networks. INTEGRATION microscopic traffic assignment and simulation software was used to evaluate the performance of the proposed controller relative to a decentralized PSC optimization controller and a fully-coordinated adaptive PSCO optimization controller in the town of Blacksburg, VA, and in downtown Los Angeles, CA.

Several simulations were conducted on the Blacksburg network using different threat point values to determine their effect on the DNB controller's performance. The results showed significant reductions on the network in the average total delay of 19.3% and 22.6%, a reduction in the stopped delay of 51% and 61%, a reduction in the average travel time of 6.1% and 7.3%, and a reduction in the emission levels of 3.8% and 3.7% over the PSC and PSCO controllers, respectively. In addition, the results showed significant reductions at the intersection links in the average travel time of 23.6%, a reduction in the average queue length of 37.6%, a reduction in the average number of stops of 23.6%, a reduction in the Co_2 emitted of 10.4%, a reduction in fuel consumption of 9.8%, and a reduction in NO_X emitted of 5.4%. The DNB

controller's performance was also tested on a downtown Los Angeles, CA network and compared to the performance of a PSC controller. The results showed significant reductions on the network in the average total delay of 14.5%, a reduction in the stopped delay of 25.1%, a reduction in the average travel time of 8%, a reduction in the average number of stops of 12.4% and a reduction in the Co_2 emitted of 4.25% over the PSC controller. Moreover, the results showed significant reductions on the intersection links in the average travel time of 35.1%, a reduction in the average queue length of 54.7%, a reduction in the average number of stops of 44%, a reduction in the Co_2 emitted of 10%, a reduction in the fuel consumption of 10%, and a reduction in $\mathrm{NO_X}$ emitted of 11.7%. Furthermore, simulations were conducted at lower traffic flow, and results showed significant reductions on the network in the average total delay of 36.7%, a reduction in the stopped delay of 90.2%, and a reduction in the average number of stops of 35% over the PSC controller, indicating that the DNB controller can generate major performance improvements at lower demands.

The results of this work showed significant potential benefits of using the proposed DNB controller over other state-of-the-art centralized and decentralized controllers on large scale networks. This research presented a novel traffic signal controller that is able to adapt signal plans based on the observed traffic state without using historical data. The developed control system is decentralized, which will increase both its scalability and robustness. The proposed controller was evaluated on traffic scenarios that represent those found in the real world, which ensures that the controller is applicable to real-life situations. The proposed DNB controller is capable of alleviating congestion as well as reducing emissions and enhancing air quality.

References

[1] M. I. Elbakary, H. M. Abdelghaffar, K. Afrifa, H. A. Rakha, M. Cetin, and K. M. Iftekharuddin. Aerosol detection using lidar-based atmospheric profiling. *SPIE Optics & Photonics*, 2017.

[2] Cebr. The future economic and environmental costs of gridlock in 2030. Technical report, Center for Economics and Business Research, July 2014.

[3] Y. Dai, D. Zhao, and Z. Zhang. Computational intelligence in urban traffic signal control: A survey. *IEEE Transactions on Systems, Man, and Cybernetics*, 42(4):485–494, July 2012.

[4] R. P. Roess, E. S. Prassas, and W. R. McShane. *Traffic Engineering - Fourth Edition*. Pearson Prentice Hall, 2010.

[5] L. J. French and M. S. French. Benefits of signal timing optimization and its to corridor operations. Technical report, French Engineering, LLC, August 2006.

[6] P. B. Hunt, D. I. Robertson, R. D. Bretherton, and R. I. Winton. Scoot-a traffic responsive method of coordinating signals. Technical report, Transport and Road Research Laboratory, 1981.

[7] A. G. Sims and K. W. Dobinson. Scat-the sydney coordinated adaptive traffic system philosophy and benefits. *International Symposium on Traffic Control Systems*, 1979.

[8] K. L. Head, P. B. Mirchandani, and D. Sheppard. Hierarchical framework for real-time traffic contro. *Transportation Research Record*, 1360:82–88, 1992.

[9] N. H. Gartner. Opac: A demand-responsive strategy for traffic signal control. *Transportation Research Record: Journal of the Transportation Research Board*, 906:75–81, 1983.

[10] M. R. Evans. Balancing safety and capacity in an adaptive signal control system - phase 1. Technical report, OFederal Highway Administration, October 2010.

[11] K. Iftekharuddin, M. Elbakary, K. Afrifa, M. Cetin, H. Rakha, and H. M. Abdelghaffar. Lidar for air quality measurement. Technical report, Mid-Atlantic Transportation Sustainability University Transportation Center, University of Virginia, January 2017.

[12] S. Tantawy, B. Abdulhai, and H. Abdelgawad. Multiagent reinforcement learning for integrated network of adaptive traffic signal controllers. In *IEEE transactions on intelligent transportation systems*, 2013.

[13] J. Chen. Game-theoretic formulations of interaction between dynamic traffic control and dynamic traffic assignment. *Transportation Research Record*, 1617:179–188, 1998.

[14] L. Jun. Study on game-theory-based integration model for traffic control and route guidance. In *Tian Jin University.*, 2003.

[15] Z. Han, D. Niyato, W. Saad, T. Basar, and A. Hjorungnes. *Game Theory in Wireless and Communication Networks: Theory, Models, and Applications*. Cambridge University Press, New York, 2012.

[16] G. Lai, C. Li, K. Sycara, and J. Giampapa. Literature review on multi-attribute negotiations. Technical report, Carnegie Mellon University, Robotics Institute, December 2004.

[17] H. Park and M. van. Bargaining strategies for networked multimedia resource management. *IEEE Transactions on Signal Process*, 55:496–3511, 2007.

[18] Z. Han and K. J. R. Liu. Fair multiuser channel allocation for ofdma networks using nash bargaining solutions and coalitions. *Communications, IEEE Transactions*, 53:1366–1376, August 2005.

[19] Z. Zhang, H. Hwa Chen, M. Guizani, and P. Qiu. A cooperation strategy based on nash bargaining solution in cooperative relay networks. *Vehicular Technology, IEEE Transactions*, 57:2570–2577, July 2008.

[20] P. A. Grout. Investment and wages in the absence of binding contracts: A nash bargaining approach. *Econometrica: Journal of the Econometric Society*, pages 449–460, 1984.

[21] I. M. McDonald and R. M. Solow. Wage bargaining and employment. *The American Economic Review*, pages 896–908, 1981.

[22] E. Larsson and E. Jorswieck. Competition versus cooperation on the miso interference channel. *IEEE Journal on Selected Areas in Communications*, 26:1059–1069, 2008.

[23] M. Van Aerde and H. A. Rakha. Realtran: An off-line emulator for estimating the impacts of scoot. *Transportation Research Record*, (1494):124–128, 1995.

[24] H. A. Rakha, M. Van Aerde, and E.R. Experiments in incremental real-time optimization of phase, cycle, and offset times using an on-line adaptation of transyt-7f. In *Engineering Foundation Conference on Traffic Management: Issues and Techniques*, Palm Coast, Florida, April 1991.

[25] M. Van Aerde and Hesham A. Rakha. Integration c release 2.40 for windows: User's guide – volume i: Fundamental model features. Technical report, October 2012.

[26] M. Van Aerde and Hesham A. Rakha. Integration release 2.40 for windows: User's guide-volume ii: Advanced model features. Technical report, June 2013.

[27] Hesham A Rakha and Yihua Zhang. The integration 2.30 framework for modeling lane-changing behavior in weaving sections. *Transportation Research Record: Journal of the Transportation Research Board*, 1883(140-149), 2004.

[28] Hesham A Rakha, Praveen Pasumarthy, and Slimane Adjerid. A simplified behavioral vehicle longitudinal motion model. *Transportation Letters: The International Journal of Transportation Research*, 1(2):95–110, 2009.

[29] Hesham A Rakha. Validation of van aerde's simplified steady-state car-following and traffic stream model. *Transportation Letters: The International Journal of Transportation Research*, 1(13):227–244, 2009.

[30] N Wu and Hesham A Rakha. Derivation of van aerde traffic stream model from tandem-queueing theory. *Transportation Research Record: Journal of the Transportation Research Board*, 2124(18-27), 2009.

[31] Hesham A Rakha, Ivana Lucic, Sergio Demarchi, and Jose Setti. Vehicle dynamics model for predicting maximum truck accelerations. *Journal of Transportation Engineering*, 127(5):418–425, 2001.

[32] Hesham A Rakha, Matthew Snare, and Francois Dion. Vehicle dynamics model for estimating maximum light duty vehicle acceleration levels. *Transportation Research Record: Journal of the Transportation Research Board*, 1883(40-49), 2004.

[33] Francois Dion, Hesham A Rakha, and Yoon So Kang. Comparison of delay estimates at under-saturated and over-saturated pre-timed signalized intersections. *Transportation Research, Part B: Methodological*, 38(2):99–122, 2004.

[34] Hesham A Rakha, Yoon So Kang, and Francois Dion. Estimating vehicle stops at under-saturated and over-saturated fixed-time signalized intersections. *Transportation Research Record*, 1776:128–137, 2001.

[35] Kyoungho Ahn, Hesham A Rakha, Antonio Trani, and Michel Van Aerde. Estimating vehicle fuel consumption and emissions based on instantaneous speed and acceleration levels. *Journal of Transportation Engineering*, 128(2):182–190, 2002.

[36] Hesham A Rakha, Kyoungho Ahn, and Antonio Trani. Development of vt-micro framework for estimating hot stabilized light duty vehicle and truck emissions. *Transportation Research, Part D: Transport & Environment*, 9(1):49–74, 2004.

[37] Hesham A Rakha and Kyoungho Ahn. Integration modeling framework for estimating mobile source emissions. *Journal of Transportation Engineering*, 130(2):183–193, 2004.

[38] L. J. French and M. S. French. Benefits of signal timing optimization and its to corridor operations. Technical Report FHWA–PA-2006-007-040214-P1, The Pennsylvania Department of Transportation Bureau of Planning and Research, August 2006.

[39] Y. Shoham, R. Powers, and T. Grenager. Multi-agent reinforcement learning: A critical survey. Technical report, Computer Science Department, Stanford University, California, US, 2003.

[40] C. Daganzo. *Fundamentals of Transportation and Traffic Operations*. Emerald Group, 1997.

[41] A. M. Turky, M. S. Ahmad, M. Yusoff, and B. T. Hammad. Using genetic algorithm for traffic light control system with a pedestrian crossing. In *4th International Conference, RSKT*, Gold Coast, Australia, July 2009.

[42] X. Yang. Comparison among computer packages in providing timing plans for iowa arterial in lawrence, kansas. *Journal of Transportation Engineering*, 127:311–318, 2001.

[43] and J. Marchand M. D. Armstrong, J. R. Rhodes, A. MacNab, P. V. Godfrey, and S. Cass. Improved operation of urban transportation systems, volume 1: Traffic signal control strategies – a state-of-the-art. Technical report, Ministry of Transport, Canada.

[44] J. MacGowan and I. J. Fullerton. Development and testing of advanced control strategies in the urban traffic control system. *Public Roads*, 43:97–105., 1979.

[45] A. Gosavi. Simulation-based optimization: Parametric optimization techniques and reinforcement learning. In *Springer, Netherlands*, pages 1151–1158, 2003.

[46] M. Selinger and l. Schmidt. Adaptive traffic control systems in the united states. Technical report, HDR Engineering, Septamber 2009.

[47] B. Abdulhai, H. Porwal, and W. Recker. Short-term freeway traffic flow prediction using genetically optimized time-delay-based neural networks. In *Transportation Research Board*, Washington D.C., USA, 1999.

[48] D. M. Mukhopadhyay, A. Farkhod M. O. Balitanas, S. H. Jeon, and D. Bhattacharyya. Genetic algorithm:a tutorial review. *International Journal of Grid and Distributed Computing*, 2:25– 32, 2009.

[49] H. Ceylan and M. G. H. Bell. Traffic signal timing optimization based on genetic algorithm approach, including driver's routing. In *Transportation Research Part B*, volume 38, page 329–342, 2004.

[50] J. Sanchez, M. Galan, and E. Rubio. Applying a traffic lights evolutionary optimization technique to a real case. *IEEE Transactions on Evolutionary Computation*, 12:25–40, 2008.

[51] H.G. Beyer and H.P. Schwefel. Evolution strategies - a comprehensive introduction. *Natural Computing*, 1:3–25, 2002.

[52] Y.K. Chin, K.C. Yong, N. Bolong, S.S. Yang, and K.T.K. Teo. Multiple intersections traffic signal timing optimization with genetic algorithm. In *IEEE International Conference on Control System, Computing and Engineering*, 2011.

[53] A. Vogel, C. Goerick, and W. V. Seelen. Evolutionary algorithms for optimizing traffic signal operation. In *European Symposium on Intelligent Techniques*, 2000.

[54] Z. Liu. A survey of intelligence methods in urban traffic signal control. *International Journal of Computer Science and Network Security*, 7:105–112, 2007.

[55] H. Ceylan and M. Bell. Traffic signal timing optimisation based on genetic algorithm approach, including drivers' routing. In *Transportation Research Part B Methodology*, May 2004.

[56] L.A. Zadeh. Fuzzy logic: computing with words. *IEEE Transactions on Fuzzy Systems*, 4, 1996.

[57] C. P. Pappis and E. H. Mamdani. A fuzzy logic controller for a traffic junction systems. *IEEE Transactions on Man and Cybernetics*, 7:707–717, 1977.

[58] S. Chiu and S. Chand. Self-organizing traffic control via fuzzy logic. In *32nd IEEE Conference In Decision and Control*, pages 1897–1902, 1993.

[59] J.C. Spall and D.C. Chin. A model-free approach to optimal signal light timing for system-wide traffic control. In IEEE, editor, *33rd IEEE Conference on Decision and Control*, number 1868-1875, 1994.

[60] D. Srinivasan, M. C. Choy, and R. L. Cheu. Neural networks for real-time traffic signal control. *IEEE Transactions on Intelligent Transportation Systems*, 7, September 2006.

[61] R. S. Sutton and A. G. Barto. *Reinforcement Learning: An Introduction*. The MIT Press Cambridge, Massachusetts London, England, 2012.

[62] M.A. Wiering, J. Vreeken, J. Van Veenen, and A. Koopman. Simulation and optimization of traffic in a city. *Intelligent Vehicles Symposium*, pages 453–458, 2004.

[63] M.A. Wiering. Multi-agent reinforcement learning for traffic light control. In *Seventeenth International Conference on Machine Learning*, pages 1151–1158, 2000.

[64] B. Abdulhai, R. Pringle, and G. J. Karakoulas. Reinforcement learning for true adaptive traffic signal control. *Journal of Transportation Engineering*, 129:278–285, 2003.

[65] A. Salkham, R. Cunningham, A. Garg, and V. Cahill. A collaborative reinforcement learning approach to urban traffic control optimization. In *International Conference on Web Intelligence and Intelligent Agent Technology*, 2008.

[66] M. K. Ekbatani, A. Kouvelas, I. Papamichail, and M. Papageorgiou. Exploiting the fundamental diagram of urban networks for feedback-based gating. *Transportation Research Part B*, page 1393–1403, 2012.

[67] M. K. Ekbatani, M.s Papageorgiou, and V. L. Knoop. Controller design for gating traffic control in presence of time-delay in urban road networks. *Transportation Research Part C*, pages 308–322, 2015.

[68] K. K. Yit, P. Rajendran, and L. K. Wee. Proportional-derivative linear quadratic regulator controller design for improved longitudinal motion control of unmanned aerial vehicles. *International Journal of Micro Air Vehicles*, pages 41–50, 2016.

[69] N. Hashimoto, U.Ozguner, and N. Sawant. Evaluation of control in a convoy scenario lqr-based sequential state feedback controller. In *IEEE Intelligent Vehicles Symposium*, Baden-Baden, Germany, June 2011.

[70] K. Aboudolas, M. Papageorgiou, and E. Kosmatopoulos. Control and optimization methods for traffic signal control in large-scale congested urban road networks. In *American Control Conference*, New York City, USA, July 2007.

[71] M. J. Osborne and A. Rubinstein. *A Course in Game Theory*. Massachusetts Institute of Technology, 2011.

[72] H. M. Abdelghaffar, H. Yang, and H. A. Rakha. Isolated traffic signal control using a game theoretic framework. In *IEEE 19th International Conference on Intelligent Transportation Systems (ITSC)*, pages 1496–1501, Nov 2016.

[73] P. Holm, D. Tomich, J. Sloboden, and C. Lowrance. Traffic analysis toolbox: Guidelines for applying corsim microsimulation modeling software. Technical report, Office of Operations Federal Highway Administration, January 2007.

[74] H. M. Abdelghaffar, H. Yang, and H. A. Rakha. Isolated traffic signal control using nash bargaining optimization. *Global Journal of Researches in Engineering: B Automotive Engineering*, 16:27–36, 2016.

[75] E. Camponogara and W. Kraus. Distributed learning agents in urban traffic control. In *11th Portuguese Conference on Artificial Intelligence*, 2003.

[76] D. Oliveira and A. Bazzan. Reinforcement learning-based control of traffic lights in non-stationary environments. In *Fourth European Workshop on Multi-Agent Systems*, 2006.

[77] S. El-Tantawy and B. Abdulhai. An agent-based learning towards decentralized and coordinated traffic signal control. In *Annual Conference on Intelligent Transportation Systems*, Madeira Island, Portugal, September 2010.

[78] S. El-Tantawy, B. Abdulhai, and H. Abdelgawad. Design of reinforcement learning parameters for seamless application of adaptive traffic signal control. *Intelligent Transportation Systems: Technology, Planning, and Operations*, 18:227–245, July 2014.

[79] H. M. Abdelghaffar, H. Yang, and H. A. Rakha. A novel game theoretic de-centralized traffic signal controller: Model development and testing. In 97*th Transportation Research Board Annual Meeting*, Washington DC, January 2018.

[80] J. Sangster and H. Rakha. Enhancing and calibrating the rakha- pasumarthy-adjerid car-following model using naturalistic driving data. *Transportation Science and Technology*, 3:229–248, 2014.

[81] M. Van Aerde and Hesham A. Rakha. Queensod rel. 2.10 - user's guide: Estimating origin - destination traffic demands from link flow counts. Technical report, March 2010.

[82] H. M. Abdelghaffar, H. Yang, and H. A. Rakha. Developing a de-centralized cycle-free nash bargaining arterial traffic signal controller. In 5^{th} *IEEE International Conference on Models and Technologies for Intelligent Transportation Systems*, pages 544 – 549, June 2017.

[83] H. M. Abdelghaffar and H. A. Rakha. A novel decentralized game-theoretic adaptive traffic signal controller: Large-scale testing. *Sensors*, 19(10), 2019.

[84] J. Du, H. A. Rakha, A. Elbery, and M. Klenk. Microscopic simulation and calibration of a large-scale metropolitan network: Issues and proposed solutions. In *97th Annual Meeting of Transportation Research Board*, Washington DC, USA, January 2018.